OPEN

# Summating Potential as Marker of Intracochlear Position in Bipolar Electrocochleography

Peter Baumhoff,[1] Laya Rahbar Nikoukar,[1] José Santos Cruz de Andrade,[1,2,3] Thomas Lenarz,[1,4] and Andrej Kral,[1,4,5]

**Objectives:** Cochlear implantation criteria include subjects with residual low-frequency hearing. To minimize implantation trauma and to avoid unwanted interactions of electric- and acoustic stimuli, it is often recommended to stop cochlear implantation before the cochlear implant (CI) reaches the cochlear partition with residual hearing, as determined by an audiogram. For this purpose, the implant can be used to record acoustically evoked signals during implantation, including cochlear compound action potentials (CAP), cochlear microphonics (CMs), and summating potentials (SPs). The former two have previously been used to monitor residual hearing in clinical settings.

**Design:** In the present study we investigated the use of intracochlear, bipolar SP recordings to determine the exact cochlear position of the contacts of implanted CIs in guinea pig cochleae (n = 13). Polarity reversals of SPs were used as a functional marker of intracochlear position. Micro computed tomography (μCT) imaging and a modified Greenwood function were used to determine the cochleotopic positions of the contacts in the cochlea. These anatomical reconstructions were used to validate the SP-based position estimates.

**Results:** The precision of the SP-based position estimation was on average within ± 0.37 octaves and was not impaired by moderate hearing loss caused by noise exposure after implantation. It is important to note that acute hearing impairment did not reduce the precision of the method. The cochleotopic position of CI accounted for ~70% of the variability of SP polarity reversals. Outliers in the dataset were associated with lateral CI positions. Last, we propose a simplified method to avoid implantation in functioning parts of the cochlea by approaching a predefined frequency region using bipolar SP recordings through a CI.

**Conclusions:** Bipolar SP recordings provide reliable information on electrode position in the cochlea. The position estimate remains reliable after moderate hearing loss. The technique presented here could be applied during CI surgery to monitor the CI approach to a predefined frequency region.

**Key words:** Cochlear implant, Electrocochleography, Guinea pig, Hearing preservation, Summating potential.

**Abbreviations:** μCT = micro computed tomography; ABR = auditory evoked brainstem response; CAP = compound action potential; CI = cochlear implant; CM = cochlear microphonics; EAS = electro-acoustic stimulation; ECochG = electrocochleography; Ft = turning frequency; SP = summating potential.

(Ear & Hearing 2023;44;118–134)

## INTRODUCTION

In recent years cochlear implant (CI) surgery has been performed on increasing numbers of implantation candidates with preserved low-frequency hearing (Von Ilberg et al. 2011; Miranda et al. 2014). In CI users a combination of electric and acoustic stimulation (EAS) has proven beneficial for speech understanding and pitch perception (Driscoll et al. 2016; Pillsbury et al. 2018; Schaefer et al. 2021). A prerequisite is the preservation of residual hearing. This can be supported by individualized surgical planning adapted to cochlear size (Pietsch et al. 2017; Schurzig et al. 2021), individualized CI electrodes (Downing 2018; Nagy et al. 2018; Iso-Mustajärvi et al. 2020; Dhanasingh & Hochmair 2021), pharmacological neuroprotection during surgery (Tan et al. 2020), improved soft surgical techniques (Lenarz et al. 2019; Lenarz et al. 2020; Yoshimura et al. 2020), intraoperative, intra- and extra-cochlear monitoring of cochlear signals by electrocochleography (ECochG; Dalbert et al. 2015; Giardina et al. 2019; Haumann et al. 2019; Lorens et al. 2019; Dalbert et al. 2021) or a combination of these methods (Reiss 2020). Intraoperative ECochG is of particular interest as it provides real-time feedback on the insertion progress (Harris et al. 2017) with information on imminent insertion trauma (Mandalà et al. 2012; Bester et al. 2020). It may also correlate with overall cochlear health (Campbell et al. 2016; Haumann et al. 2019; Canfarotta et al. 2021; Dalbert et al. 2020). Provided sufficient residual hearing, ECochG can additionally be used to assess the electrode position in the cochlea (Helmstaedter et al. 2018; Koka et al. 2018; Sijgers et al. 2021).

The ECochG signal is a superposition of multiple signals: (i) the auditory nerve neurophonic potential and (ii) the compound action potential (CAP), both originating from the auditory nerve; (iii) cochlear microphonic (CM) potential, and (iv) the summating potential (SP), generated by inner and outer hair cells and contributions by the auditory nerve (Johnstone & Johnstone 1966; Dallos 1973; van Emst et al. 1995; Sellick et al. 2003; Forgues et al. 2014; Pappa et al. 2019). The contributions of each of these components to the overall ECochG signal depend on stimulus frequency, stimulus intensity, and recording position. The whole ECochG signal and especially the CM are the focus of numerous studies in the last decade due to the prominent frequency following characteristics at low-stimulation frequencies. The CM is dominated by the transducer currents of outer hair cells with contributions from inner hair cells (Forgues

[1]Department of Experimental Otology & Institute of AudioNeuroTechnology (VIANNA), ENT Clinics, Hannover Medical School, Hannover, Germany; [2]Department of Otorhinolaryngology and Head and Neck Surgery, Federal University of São Paulo (UNIFESP), São Paulo, Brazil; [3]Coordenação de Aperfeiçoamento de Pessoal de Nível Superior (CAPES Foundation), Brasília, Brazil; [4]Cluster of Excellence "Hearing4all", Hannover, Germany; and [5]Department of Biomedical Sciences, School of Medicine and Health Sciences, Macquarie University, Sydney, Australia



Supplemental digital content is available for this article. Direct URL citations appear in the printed text and are provided in the HTML and text of this article on the journal's Web site (www.ear-hearing.com).

et al. 2014; Kamerer et al. 2016). In clinical cases, the CM is often the main contributor to the ECochG response. Changes in the signal during surgery might predict hearing preservation after cochlear implantation (Adunka et al. 2016; Dalbert et al. 2016; Harris et al. 2017; Haumann et al. 2019). Nevertheless, the relation between intraoperative findings and postoperative hearing outcomes is still inconclusive: Preservation of intraoperative potentials does not necessarily ensure postoperative hearing preservation (Haumann et al. 2019; Dalbert et al. 2020). While different criteria and definitions for electrophysiological trauma have been proposed (Giardina et al. 2019), there is no consensus on a unified approach. The results vary, and the reasons include, for example, the exact scalar location of the CI and varying implantation depth. Such biasing factors are not well understood (O'Connell et al. 2016; O'Connell et al. 2017; Sijgers et al. 2021; Dalbert et al. 2021). Because the CM shows complex variations in amplitude throughout the normal hearing cochlea (Helmstaedter et al. 2018) and the CAP does not provide reliable cochlear location information (Eggermont 1976; Brown & Patuzzi 2010), in the present study we focused on SPs. The SP can be reliably recorded in human cochleae, including in CI candidates (Pappa et al. 2019), even though it appears to be rather small in many cases.

While hearing preservation in deep implantation has been previously demonstrated (Yoshimura et al. 2020), an overlap between electric and acoustic stimulation may affect speech recognition by masking effects between the acoustic and electric stimulation (Krüger et al. 2017; Imsiecke et al. 2020). Knowledge about the intracochlear electrode position could provide valuable information for adjusting the implantation depth, for example, by avoiding implantation into the hearing part of the cochlea through partial insertion (Lenarz et al. 2019). This could both prevent loss of residual hearing and minimize masking effects between electric and acoustic stimuli.

We have previously suggested the SP as a potential marker of intracochlear electrode position (Helmstaedter et al. 2018). The SP is a direct current component of the ECochG signal (Dalbert et al. 2021), mainly generated by inner and outer hair cells, with contribution of a sustained potential from the auditory nerve (van Emst et al. 1995; Sellick et al. 2003; Forgues et al. 2014; Pappa et al. 2019). The SP is characterized by a sharp frequency tuning (Dallos 1973; Cheatham & Dallos 1984).

Here we present an improved bipolar ECochG recording technique to assess the cochlear location of the recording electrode. We validate it using (i) micro computed tomography (μCT) imaging and (ii) hearing-impaired ears. For this purpose we recorded the bipolar, intracochlear ECochG from five contact pairs of a custom-made six-contact CI in hearing guinea pigs. After implantation with preserved normal hearing, recordings with different electrode pairs were performed under tonal acoustic stimulation. The CI was kept in place for intracochlear and extracochlear recordings before and after noise exposure. A bipolar recording configuration was used to better localize the generators of SPs. A bipolar configuration provides signals free from far fields and allows a more exact, unbiased assessment of the local excitation in the cochlea compared with monopolar recordings (Helmstaedter et al. 2018). We hypothesized a polarity reversal of the SP occurring when the spatial position of the signal generators shifted relative to the position of the recording electrodes. The stimulation frequency at which the polarity of the SP reversed for a given recording position was defined as "turning frequency" (Ft). The results show that it corresponds to the cochlear location of the recording electrodes defined by μCTs.

To assess the robustness of the method with respect to hearing loss, an acute noise trauma (likely a mixture of temporary and permanent threshold shifts (Eggermont 2017)) was induced and the assessments of Ft were repeated. The results suggest that the method can be used also in cochleae with hearing loss. We finally suggest a procedure of SP tracking relative to a predefined frequency range in a clinical setting that assists in avoiding penetration of the CI into cochlear partitions that are of clinical relevance for EAS.

## MATERIALS AND METHODS

### Animals Model and Ethics

We used 10 male Hartley (Crl:HA) guinea pigs from Charles River Laboratories International Inc. (Écully/France) with mean weight of 411 g ± 43 g (340–750 g). All experimental procedures were in accordance with the German and European Union guidelines for animal welfare (ETS 123, Directive 2010/63/EU), and were approved by the German state authority (Lower Saxony state office for consumer protection and food safety, LAVES; approval No. 14/1514) and were monitored by the institute's animal welfare officer. Included in this study were 13 cochleae (7 left and 6 right) of 7 animals, of which μCT datasets were acquired post-mortem. At the beginning of the procedure, the auditory status of the animals was screened with auditory brainstem response (ABR) measurements. All animals had a normal hearing threshold defined as click-evoked ABR-thresholds equal to or below 35 dB peak equivalent SPL (peSPL).

### Study Design

We monitored the cochlear function by extra-cochlear CAP recordings in 13 cochleae before and after cochleostomy and CI insertion. Subsequently, we recorded ECochG in a bipolar recording configuration from neighboring contacts of the implant for a total of 61 intracochlear recording positions (9 full CI insertions and 4 shallow CI insertions of 5 contacts). The implant was kept in place throughout the experiments. The amplitude of the SP for frequencies between 2 kHz and 32 kHz at multiple supra-threshold sound levels was analyzed for all recording positions and the stimulation frequency at which the SP polarity reversed (Ft) for the given electrode contact was identified. Subsequently, a cochlear trauma was induced by noise exposure at high sound levels. All electrophysiological recordings were repeated afterward. For validation of the results, in all 13 cochleae, the CI position was assessed using post-mortem μCT imaging. The tonotopic positions of the CI contacts, as well as the positions of the midpoints between contacts, were reconstructed according to the formula introduced by Tsuji and Liberman (1997). The Ft as an electrophysiological measure of the tonotopic recording position was compared with the reconstructed midpoint frequencies from μCTs. A schematic overview of all interventions and measurements can be found in Figure 1A.

### Anesthesia and Monitoring

Anesthesia was induced by intramuscular injection of 50 mg/kg body weight ketamine (CP Pharma, Burgdorf, Germany) and

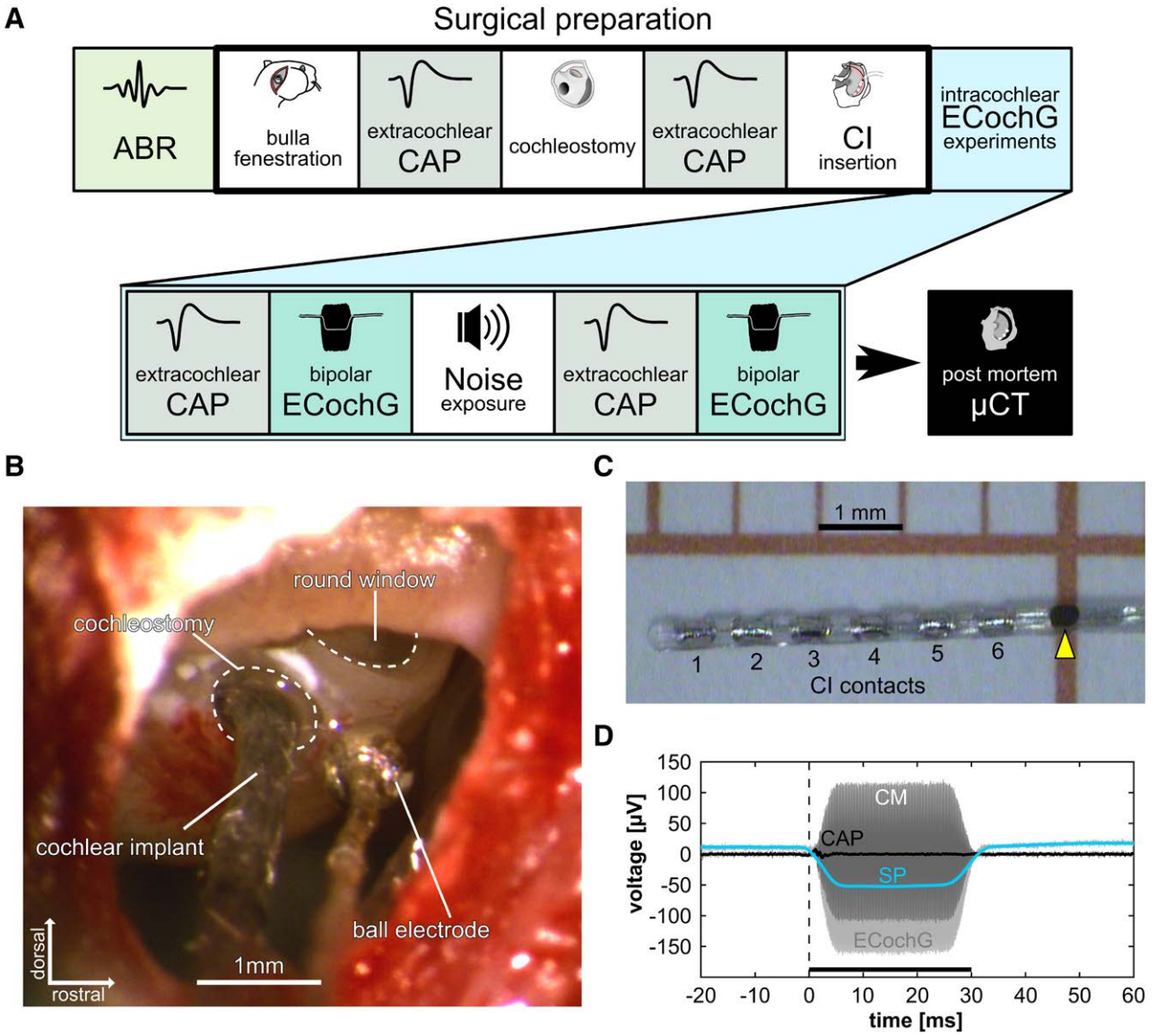


Fig. 1. Intra- and extra-cochlear recordings were combined to access the summating potential (SP) locally while monitoring cochlear function globally by compound action potential (CAP) recordings. A, Workflow diagram of all interventions and measurements during the experiments. B, Exemplary surgical view on the basal cochlear turn. A retroauricular fenestration in the tympanic bulla gives access to the cochlear base. A cochlear implant (CI) for intracochlear electro cochleography (ECochG) recordings was inserted through a cochleostomy below the round window edge. A silver ball electrode was placed on the lateral wall of the cochlear base close to the cochleostomy for CAP recordings. C, We used custom made guinea pig CIs (MedEl, Insbruck, Austria) with 6 contacts (700 µm spacing) of the depicted type. The distance between the centers of the most basal and the most apical contact was 3.5 mm. The implants were 5 mm long from tip to insertion marker (yellow arrowhead). D, The ECochG was filtered to separate the compound action potential (CAP), the cochlear microphonic (CM) signal, and the summation potential (SP). The SP amplitude was determined for further analysis. The dashed line marks the stimulus onset and the black line at the bottom indicates the stimulus duration.

10 mg/kg xylazine (WDT, Garbsen, Germany). 0.1 mg/kg atropine sulfate (B. Braun Melsungen AG, Melsungen, Germany) was additionally applied with anesthetics to reduce bronchial secretion. For maintenance of anesthesia, 25 to 30% of the initial dose without atropine sulfate was applied as required. Vital signs of the animal were monitored continuously. Corneal and paw withdrawal reflexes were tested regularly throughout the procedure to ensure an adequate depth of anesthesia. Heart rate was monitored by EKG (Otoconsult, Frankfurt a.M., Germany). Body core temperature was measured via rectal probe and maintained at approximately 38°C using a feedback-controlled heating pad (TC-1000 Temperature Controller, CWE Inc., Ardmore, USA). At the beginning of the surgery, a tracheotomy was performed. Artificial ventilation was applied using a rodent ventilator (Rodent Ventilator 7025, Ugo Basile, Comerio, Italy). The respiratory rate was set between 40 and 60 breaths per minute and the end-tidal $CO_2$ concentration was continuously monitored (Normocap $CO_2$ & $O_2$ Monitor, Datex, Helsinki, Finland).

### Surgical Procedure

All the subsequent procedures and measurements were carried out in a sound-proof, anechoic chamber. The head of the anesthetized animal was secured in a customized rodent head holder that allowed adjustment along three axes. After

administration of local anesthetics (2% Lidocaine) onto the skin, the pinna was resected. The postero-lateral surface of the tympanic bulla was exposed by dissection of the overlying soft tissue. Under microscopic control (Carl Zeiss OPMI-1, Carl Zeiss, Goettingen, Germany) the bulla was opened with a hollow needle and the lateral wall was carefully removed until the middle ear and the round window niche were exposed. Then a silver ball electrode was placed on the outer wall of the basal cochlear turn (Fig. 1B) with a micromanipulator. A cochleostomy was drilled in the basal turn of the cochlea, centered at approximately 0.5 mm below and latero-caudal from the round window (Fig. 1B) using a 0.6 mm diamond burr. A moderate drilling speed (4000 rpm) was chosen to avoid noise trauma. The CI was then inserted through the cochleostomy either until five contacts were inserted or until first resistance was felt (full insertion). After insertion, the silastic carrier of the CI was fixed to the bony wall of the bulla using tissue adhesive (Histoacryl; B. Braun Melsungen AG). At the end of the experiment, the animals were euthanized under deep anesthesia by intra-cardiac infusion of 2 mL sodium pentobarbital (Release, WDT eG, Garbsen, Germany), and the heads were fixed in 3.5 to 3.7% buffered formaldehyde solution for post mortem μCT scans.

### Cochlear Implant

Custom-designed guinea pig CIs with a diameter of 500 μm tapering to 300 μm at the tip (Med-El Inc., Innsbruck, Austria) was used in this study. Each CI had six platinum contacts spaced by 700 μm center to center. A black insertion marker positioned approximately 1 mm behind the basal contact served as an orientation during insertion (Fig. 1C).

### Auditory Brainstem Response Recordings

To screen the animals' hearing status, click-evoked ABRs were recorded from three transcutaneous silver wire electrodes before the surgery. The active electrode was inserted at vertex, the reference electrode posterior to the tested ear, and the ground electrode in the neck. An audiometric headphone speaker (DT48, Beyerdynamic, Heilbronn, Germany) was placed approximately 3 cm from the ipsilateral ear (near free-field condition). Acoustic stimuli were generated digitally by a stimulation and data acquisition software (AudiologyLab, Otoconsult), and responses were acquired by a two-channel recording setup (Otoconsult). Stimulus generation was controlled by a 96-channel digital I/O card (PCIe-6509 DIO, National Instruments, Austin, TX, USA). Stimulations were 50-μs condensation clicks of increasing intensity from 0 to 80 dB peSPL (5 dB steps). Response signals were amplified by 100 dB ($\times 10^5$) and filtered between 200 Hz and 5 kHz (sixth-order Butterworth filter, 12 dB/octave) and recorded through a 32-channel MIO card (PCI-6259, National Instruments) at a sampling rate of 100 kHz. The signals were averaged over 100 repetitions. Normal hearing was defined as click-evoked ABR-threshold 35 dB peSPL or lower.

### Extracochlear CAP Recordings

CAPs were recorded through the silver ball electrode at the outer cochlear wall to assess audiograms before cochleostomy, after cochleostomy, after CI implantation, and after induction of noise trauma. The same recording setup as for ABR recordings was used. The loudspeaker was calibrated for the stimulation range using a ¼-inch condenser microphone (type 4939, Brüel & Kjaer, Nærum, Denmark) connected to a preamplifier (type 2670, Brüel&Kjaer) and a conditioning amplifier (type 2690, Nexus conditioning amplifier, Brüel & Kjaer). The signals were recorded through an MIO card at a sampling rate of 100 kHz. A custom-made PVC stimulation cone was attached to the loudspeaker and the microphone was placed in front of the cone for recording and storing a calibration curve of the speaker output. During the recordings, the loudspeaker with the attached stimulation cone was placed on the exposed cartilaginous external meatus, comprising a quasi-closed field condition. All acoustic stimuli were generated digitally as described for ABR recordings. The stimulation frequencies were adjusted to the hearing range of the animal model. For extracochlear recordings, pure tone bursts with a duration of 5 ms and rise/fall times of 2.5 ms were presented at a frequency range of 1 to 32 kHz (four steps per octave) in alternating phase over an intensity range of 0 to 90 dB SPL (10 dB steps). The stimuli were presented in randomized order with 10 repetitions per stimulus and phase. The CAP signals were recorded at a sampling rate of 100 kHz, amplified by 80 dB ($\times 10^4$) and filtered between 5 Hz and 5 kHz (sixth-order Butterworth filter, 12 dB/octave). The recorded signals were processed offline to acquire a CAP audiogram.

### Intracochlear ECochG Recordings through CI

Bipolar ECochGs were recorded sequentially from pairs of neighboring CI contacts using a custom connector and the setup described earlier for ABR and CAP recordings. On the two available recording channels, the signals of two pairs of contacts (e.g., 1–2 and 5–6) were recorded simultaneously. The apical channel of each pair (lower channel number on the CI) served as the recording electrode and the basal channel as the reference. The acoustic stimuli were pure tones of 30 ms duration and 5 ms rise/fall times, in a frequency range of 1 kHz to 32 kHz (four steps per octave) and intensities of 0 to 80 dB SPL (10 dB steps). Stimuli were presented in alternating phase with 10 repetitions per stimulus and phase. The response signals were recorded at a sampling rate of 100 kHz, amplified by 40 dB ($\times 10^3$), and high-pass filtered at 2 Hz (sixth-order Butterworth filter, 12 dB/octave). The recorded signals were processed offline to extract and analyze the SP of the ECochG (Fig. 1D).

### Noise Exposure

Threshold shifts at cochleotopic positions were induced by exposure to band-filtered noise. The noise bands of 8 to 12 kHz (n = 9) and 14 to 18 kHz (n = 4) were chosen to cause threshold shifts at the basal (low frequency) or apical (high frequency) end of the inserted CI. The anesthetized animals were exposed for 1 hour to noise bands at an average of 110 dB SPL with the CI in place. The noise stimuli were generated in an open-source digital audio editor (Audacity[1] version 2.1.1). The filters had a roll-off of 36 dB per octave. Ramps with 10 s rise/fall times were added to avoid impulse responses. Signals were verified for constant output levels before and after exposure using a calibrated Bruel & Kjaer ¼ inch microphone in closed field conditions.

[1]Audacity(R) software is copyright (c) 1999-2016 Audacity Team. [Web site: http://audacityteam.org/. It is free software distributed under the terms of the GNU General Public License.] The name Audacity(R) is a registered trademark of Dominic Mazzoni.

### Micro Computed Tomography and 3-Dimensional Reconstruction

Postmortem imaging was performed on 13 implanted cochleae with a high-resolution peripheral quantitative computed tomography (μCT, Xtreme CT II, SCANCO Medical AG, Brüttisellen, Switzerland) set at 68 kVp, 1470 μA, 100 W, and voxel size of 17 μm. The DICOM images were processed using a scientific visualization platform (Amira, Version 6.0–Version 6.5, FEI Visualization Sciences Group, Bordeaux, France) for 3-dimensional reconstruction and analysis.

All implanted cochleae were registered onto μCT images of a macerated, intact left template cochlea. The reference length of the basilar membrane was constructed by tracing the midpoint between osseous spiral lamina and spiral ligament in the high-contrast template (Fig. 2A, osl-edge). The CI electrodes were traced using Amira's filament module for linear tracing between contacts (Fig. 2B, C). From the respective data, the midpoints of neighboring contacts were calculated (Fig. 2D). The spatial coordinates of the midpoints were used to calculate the relative distance of each contact to the approximate end of the basilar membrane (bm, apical end of the osl-edge). The distance from the apex was expressed as percent of total length. From this the Greenwood position frequency was calculated by the adjusted equation for the guinea pig (Tsuji & Liberman 1997) as follows:

$$F = 0.132 \times 10^{2.63x} \quad (1)$$

where F is the frequency (kHz) and $x$ is the relative distance to apex. A comparison between our positional data, the original Greenwood function (Greenwood 1990), and the adjusted Tsuji and Liberman function are provided as supplement (See Figure 1 in Supplemental Digital Content 1, http://links.lww.com/EANDH/B38). To account for the direction of CI insertion, we inverted the values to express the intra-cochlear CI position as "distance from base" in contrast with the "distance from apex" used by Greenwood, Tsuji, and Liberman.

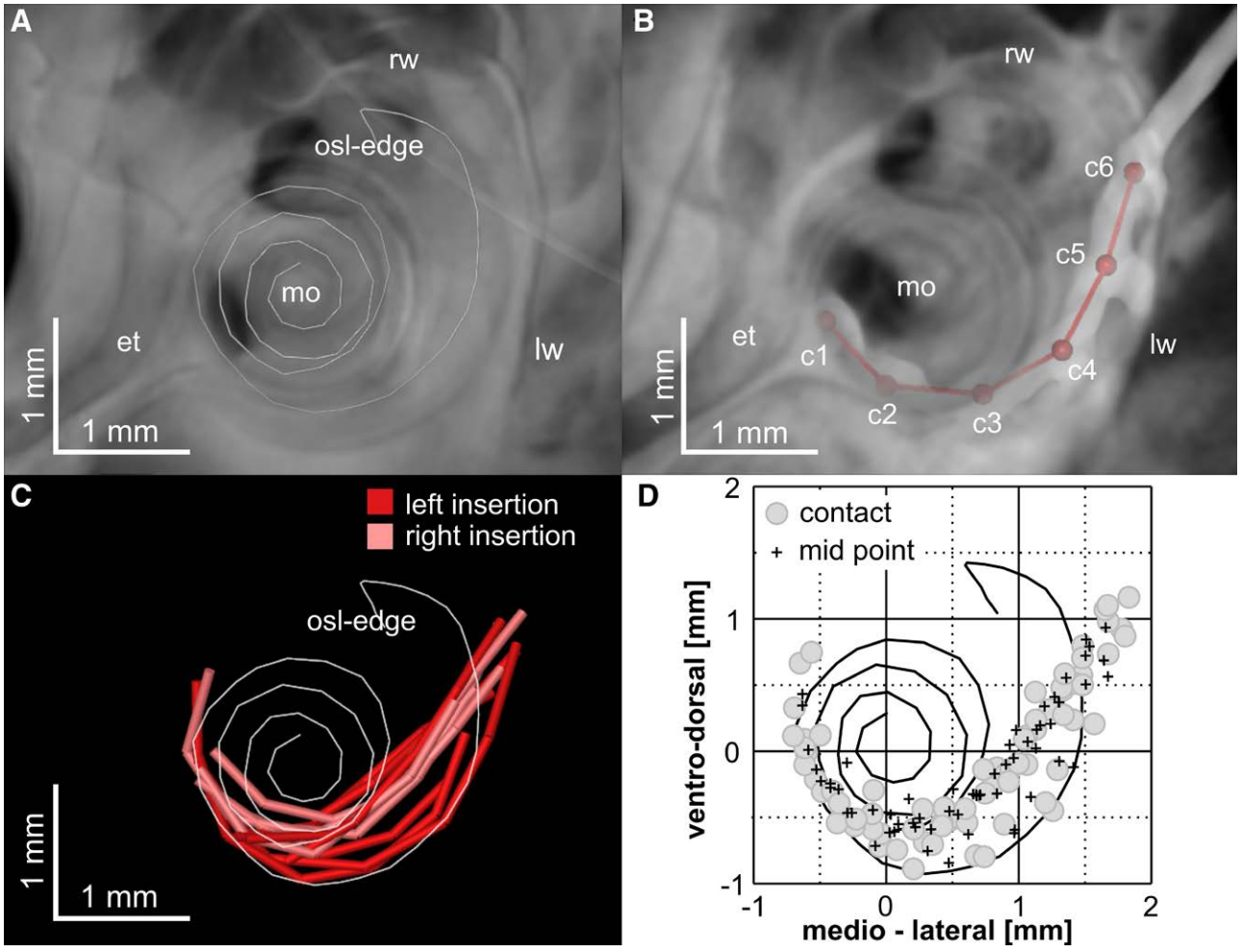


Fig. 2. Validation of the functional data using anatomical cochlear reconstruction. A, First, the length of the cochlea was estimated along the edge of the osseous spiral lamina (osl) in micro computed tomographic (μCT) images of a non-implanted left template cochlea. B, Second, an implanted study case was registered onto the template cochlea. Image stacks of right cochleae were mirrored before registration. Markers were placed onto the CI contacts (c1, c2,…, c6). C, For all 13 study cases the contact positions (not shown) and insertion paths were three dimensionally related to the template osl length. The insertion depths and angles were then determined. D, To obtain an estimate of the bipolar recording positions (n = 61), the midpoints between neighboring contacts were calculated. For a full insertion this reconstruction resulted in 5 midpoint positions. The corresponding frequency information was calculated according to the reconstructions by Tsuji and Liberman (1997). CI indicates cochlear implant; et, Eustachian tube; lw, lateral wall of the basal turn; mo, modiolus; osl, osseous spiral lamina; rw, round window.

### Data Analysis

The recorded signals were processed offline with custom-made Matlab routines (The MathWorks Inc., Natick, Massachusetts, US) to separate the response components. Extracochlear CAPs were derived offline by filtering between 0.2 kHz and 2 kHz. The peak-to-peak amplitude of the first negative and positive components of the CAP ($N_1$–$P_1$) was computed within the first 5 ms after stimulation onset. A background correction was applied, based on the peak-to-peak amplitude of a 10-ms time window before stimulation. The calculations were performed for all stimulation frequencies and intensities. CAP threshold was defined as the lowest intensity at which the CAP $N_1$ to $P_1$ amplitude was more than 3 SDs above the background level.

To analyze the SP, first-order polynomic smoothing (Savitzky-Golay smoothing filter, fifth-order) with a 5-ms window was applied to the recorded ECochGs. The maximal SP amplitude was determined in a time window of 3 ms to 15 ms after stimulus onset at all investigated frequencies and intensities. After plotting the SP amplitude over stimulation frequency, we were able to identify a common pattern of changing polarity in SP amplitude from negative in lower frequencies to positive in higher frequencies. We defined turning frequency (Ft) as the frequency at which the SP amplitude changed from negative to positive. The anatomic frequency estimate was used to verify the method.

The CAP thresholds before cochleostomy, after cochleostomy, after CI insertion, and after noise trauma were tested with a two-way repeated-measures analysis of variances with Bonferroni posttest correction and *t*-tests. The results were expressed as mean ± SE of the mean (SEM) or SD as noted for each case. In all cases, *p* values below 0.05, or equivalent Bonferroni corrections, were considered significant.

## RESULTS

In the present experiments, implantation was performed through a cochleostomy. Due to the location of the round window in guinea pigs, implantation through a cochleostomy is the least traumatic approach. The cochleostomy itself did not introduce a significant shift in CAP thresholds (Fig. 3). Thresholds below 30 dB were observed between 5.7 kHz and 13.5 kHz, as expected for normal-hearing guinea pigs (Fig. 3). The lowest thresholds after drilling the cochleostomy ranged from 0 dB SPL to 30 dB SPL with an average of 17.7 (±10.1) dB SPL. The mean threshold between 2 kHz and 16 kHz was 35.7 (±7.8) dB SPL (details in Table 1). After CI insertion thresholds were slightly elevated between 5.7 kHz and 9.5 kHz (Fig. 3), resulting in a significant threshold shift of 5.7 (±8.0) dB (paired t-test, single-sided, $p = 0.012$, $t = -2.6$). The average maximal threshold shift across all 13 cases was 26.2 (±10.4) dB. After the implantation-related threshold shift, the most sensitive region of the audiogram was at 11.3 kHz to 16 kHz with average thresholds below 40 dB SPL. The implantation-related hearing loss at the tip of the implant was less pronounced for partial insertions (5 CI contacts; n = 4; Fig. 3; Table 1).

The correlation between insertion depth and threshold shifts has been reported earlier, for a total of 24 insertions of which

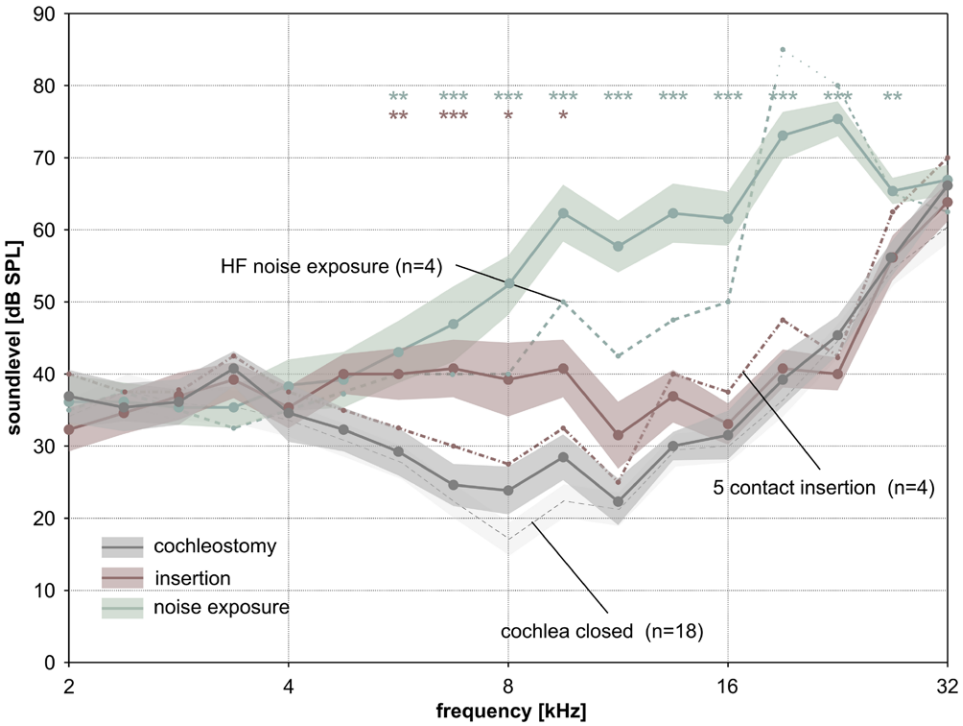


Fig. 3. Extra-cochlear CAP audiograms were recorded in all 13 cases during the experiments. The dark gray line refers to the hearing status after cochleostomy. The status before cochleostomy (n = 18) is indicated by a dashed black line and light gray shading. The lowest thresholds (average thresholds: 20 dB SPL – 30 dB SPL) were found between 5.7 kHz and 13.5 kHz. After the CI insertion, a mild but significant hearing loss could be observed between 5.7 kHz and 11.3 kHz (red line). Partial insertions in 4 cases (5 contacts inserted) led to less hearing loss (red dashed line, see also Table 1). After noise exposure (green line) the hearing loss was apparent at frequencies from 8 kHz to 26.9 kHz. In 4 cases with high-frequency noise exposure (see Materials and Methods), the largest hearing loss was restricted to 19.0 kHz - 22.6 kHz (green dashed line, see also Table 1). Shaded areas indicate ± SEM.

**TABLE 1. Hearing thresholds in all animals, are ordered by CI insertion depths**

| Animal code | Cochlear side | NT range (kHz) | Contacts inserted | Min. thres. (dB SPL) | Coch. mean (dB SPL) | Insert. shift in mean (dB) | Noise shift in mean (kHz) | Depth from base (%) | Insert. angle (°) | LMF (kHz) |
|---|---|---|---|---|---|---|---|---|---|---|
| 03K15 | Left | 8–12 | 5 | 10 | 32.3 | 2.3 | 20.8 | 30 | 111 | 10.7 |
| 03I15 | Left | 14–18 | 5 | 10 | 29.2 | 1.5 | 14.6 | 30 | 134 | 9.8 |
| 20J15 | Left | 8–12 | 5 | 30 | 38.5 | 6.2 | 18.5 | 32 | 149 | 9.2 |
| 15J15 | Left | 8–12 | 5 | 30 | 43.1 | 6.9 | 25.4 | 32 | 159 | 8.9 |
| 15J15 | Right | 8–12 | 6 | 20 | 41.5 | 4.6 | 13.8 | 34 | 186 | 7.8 |
| 29J15 | Left | 8–12 | 6 | 10 | 36.2 | 15.4 | 27.5 | 34 | 198 | 7.6 |
| 13J15 | Right | 14–18 | 6 | 10 | 25.4 | 2.3 | 17.7 | 36 | 208 | 6.9 |
| 29J15 | Right | 8–12 | 6 | 10 | 26.9 | 7.7 | 30.0 | 36 | 214 | 6.9 |
| 13J15 | Left | 14–18 | 6 | 30 | 49.2 | -5.4 | 20.0 | 36 | 223 | 6.9 |
| 05K15 | Right | 8–12 | 6 | 20 | 38.5 | 3.8 | 20.8 | 36 | 227 | 6.9 |
| 20J15 | Right | 8–12 | 6 | 0 | 25.4 | 8.5 | 30.8 | 39 | 242 | 6.1 |
| 05K15 | Left | 8–12 | 6 | 20 | 32.3 | 25.4 | 36.9 | 40 | 263 | 5.5 |
| 03I15 | Right | 14–18 | 6 | 30 | 45.4 | -4.6 | 6.2 | 42 | 270 | 4.8 |
| Mean values (SD) | | | | 17.7 (±10.1) | 35.7 (±7.8) | 5.7 (±8.0) | 21.8 (±8.2) | 35.2 (±3.7) | 198.8 (±49.1) | 7.5 (±1.7) |

*The pure tone mean threshold was calculated from 13 stimulation frequencies between 2 kHz and 16 kHz. (C1: basal contact; coch.: cochlostomy; insert.: insertion; LMF: lowest midpoint frequency; NT: noise trauma; min. thres: minimum threshold).*

the 13 cases studied here were a subset (Andrade et al. 2020). Noise exposure with band-restricted noise of either 8 kHz to 12 kHz or 14 kHz to 18 kHz (see Table 1 for details) extended the implantation-induced hearing loss with a significant elevation of thresholds up to 26.9 kHz in all 13 cases. For cases exposed to the high-frequency noise (n = 4; Fig. 3; Table 1 for details), the damage was most pronounced at 19.0 kHz and 22.9 kHz. The total average threshold shift of 21.8 (±8.2) dB was significantly above the post-insertion audiogram (paired t-test, upper-tailed, $p < 0.001$, $t = -11.3$). The maximal threshold shift was 50.8 dB (±15.0 dB). Thus, the method of partial deafening was successful.

## Intracochlear Recordings

At a fixed bipolar recording position, that is, the midpoint between neighboring CI contacts, the polarity of the SP depended on the stimulation frequency (Fig. 4A). The bipolar recording configuration (the more apical electrode referenced to the more basal electrode) typically led to negative SP polarity for acoustic stimuli at low frequencies and to positive SP polarity for high stimulation frequencies. The zero-crossing was defined as the "turning frequency" (Ft; comp. Helmstaedter et al. 2018). The Ft was recording-position-dependent (Fig. 4B). It was high for basal recording positions and low for apical recording positions. A "tilting" of the Ft along the intensity axis was apparent in the grand mean of all cases and all recording positions (Fig. 4C). The difference between the Fts at low stimulation levels compared with high stimulation levels was moderate (0.30 ± 0.30 octaves). In individual examples (Fig. 4B) as well as in the grand mean (Fig. 4C), the negative SPs at low stimulation frequencies had large amplitudes even for soft stimuli, while the positive SPs at low stimulation levels were usually close to background level. This influenced the identification of the Ft at sound levels close to the response threshold (typically at 20–30 dB SPL).

To account for individual differences in the audiogram before and after noise exposure, we compared stimulation levels relative to the level above the individual threshold. The individual threshold was defined by the minimum CAP threshold (HLs). The Fts at 10 dB HL differed significantly (n = 46 pairs, paired t-test, two-tailed, $p < 0.001$, $t = -8.57$) from the Fts at 40 dB HL, shifting the Ft to lower frequencies at higher sound levels. The hearing loss induced by noise exposure did not lead to a significant change in the Ft (Fig. 5A; two-tailed t-tests, all $p \geq 0.21$).

## Correlation between Ft and Anatomical Position Estimates

The electrophysiologically determined Ft aligned well with the anatomical estimation of the recording position, both before and after noise exposure (Fig. 5B). The majority (66%) of all Ft datapoints (n = 154 in five-sound levels, see above) deviated less than 0.5 octaves from the anatomical estimate. Considering a slope of approximately 2.6 mm/octave for the adjusted Greenwood function along the cochlear partition covered by the CI, this amounts to a distance of 1.3 mm (roughly 7% of cochlear length). As expected, only a fraction of Fts could be determined with stimulation levels close to the threshold: The inset in Figure 5B illustrates the proportions of data points with pre- and post-noise-exposure data. The highest proportion was found for 30 dB HL (Fig. 5B, inset). At 30 dB HL, the correlation between anatomical estimate and electrophysiological Ft was high, both pre noise-exposure ($R^2 = 0.72$; y = 1.04x) and post noise-exposure ($R^2 = 0.67$; y = 1.01x). In both cases, the variance in cochlear position thus accounted for approximately 70% of the variability in Ft.

## Interdependence Between Intracochlear CI Position, Insertion Trauma, and Ft Reliability

The spatial correlation between Ft (at 30 dB HL) and anatomical estimate is visualized in Figure 5C along the rostrocaudal and mediolateral axes of the basal cochlear turn. Recording positions of three CI insertions were located at an extreme lateral (abmodiolar) position compared with the majority of data points (Fig. 6A). In a separate analysis, these outliers were compared with three control insertions close to the average insertion path. The maximal insertion angles of the two groups were comparable (outliers: 198°, 223°, and 263°; controls: 214°; 242°,

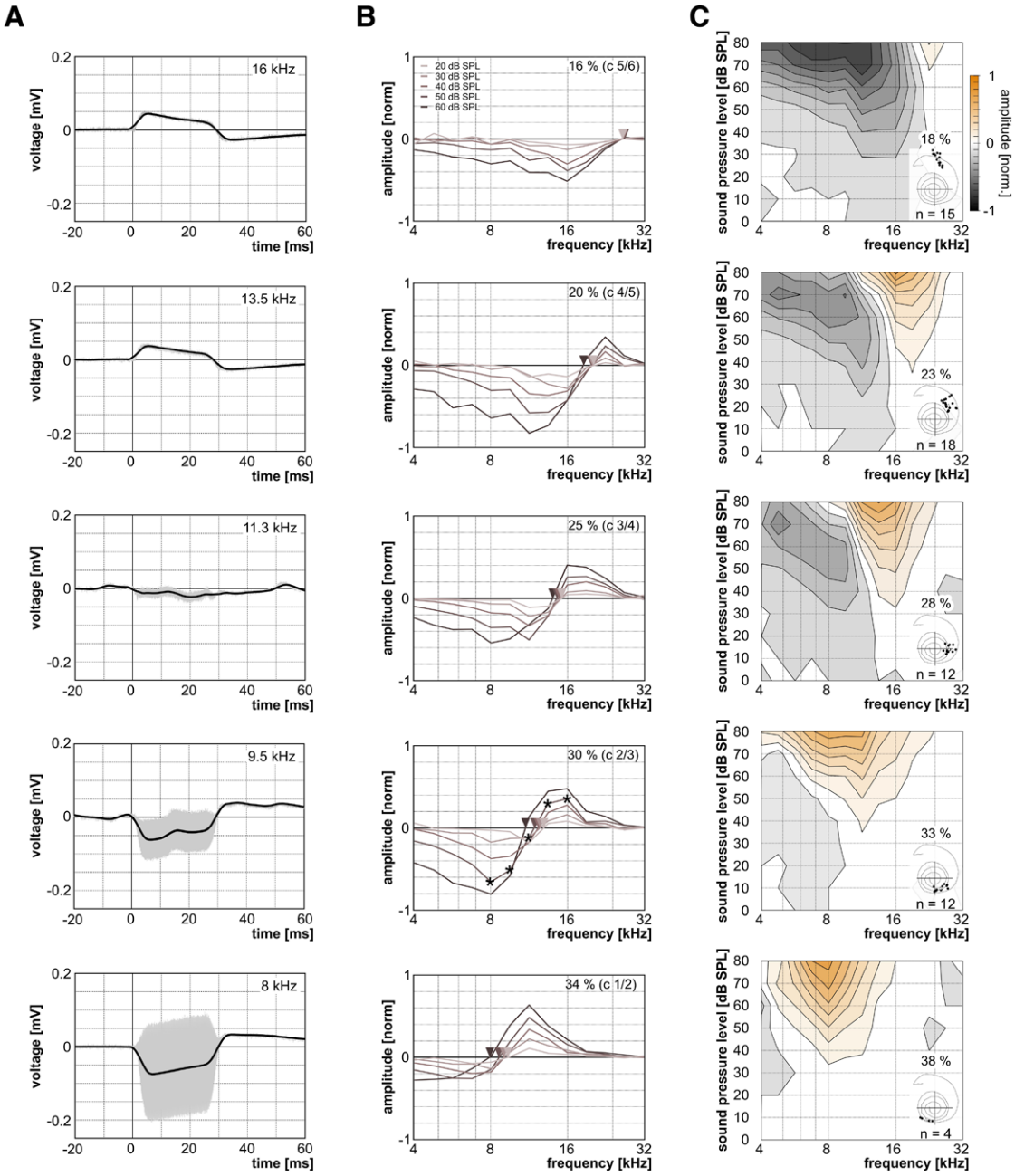


Fig. 4. The amplitude and polarity of the SP depended on the stimulation frequency and the intracochlear recording position. A, At a given recording position (bipolar c2/3) and stimulation SPL (50 dB SPL, ~30 dB HL) the polarity and amplitude of the SP (black line) depended on the stimulation frequency (inset top right) from high (top panel) to low (bottom panel). From 16 kHz to 11.3 kHz the amplitude decreased and for 9.5 kHz and 8 kHz increased again. The SP polarity switched from positive for high stimulation frequencies to negative for low stimulation frequencies. At 11.3 kHz, near the SP turning frequency (Ft), the amplitude was close to background level. The raw ECochG is depicted by the gray trace in the background. B, SP amplitudes reveal positive SP for high frequencies and negative SP for low frequencies, consistent across all recording cochlear positions (top right in each panel) except the basal-most (c5/6, 16% insertion depth from base) where only negative SP were observed for frequencies below 22.6 kHz. The SP amplitudes depicted in (A) are marked with asterisks. C, The grand mean of the pooled data of frequency-SPL dependence of normalized SP amplitudes (relative to maximum SP amplitude). Polarity reversal is consistent across stimulation levels. The insets at the lower right in each panel depict the insertion points included in the mean. Inset percentages are the average insertion depths.

and 270°). For the outliers, up to three contacts were positioned near the lateral wall (the basalmost contacts) and outside of the SDs of average insertions. In contrast, all contacts of the controls were within one SD of average insertions. A comparison of the extra-cochlear CAP data between the two groups revealed tendency for a more pronounced threshold shift for the outliers compared with the controls that persisted after noise exposure (Fig. 6B). This suggests that the abmodiolar insertion of the implant in this study may have affected the cochlear mechanics or induced more cochlear trauma.

The mean deviation from the global average threshold shift between 4.8 kHz and 11.3 kHz was 13.6 dB for outliers

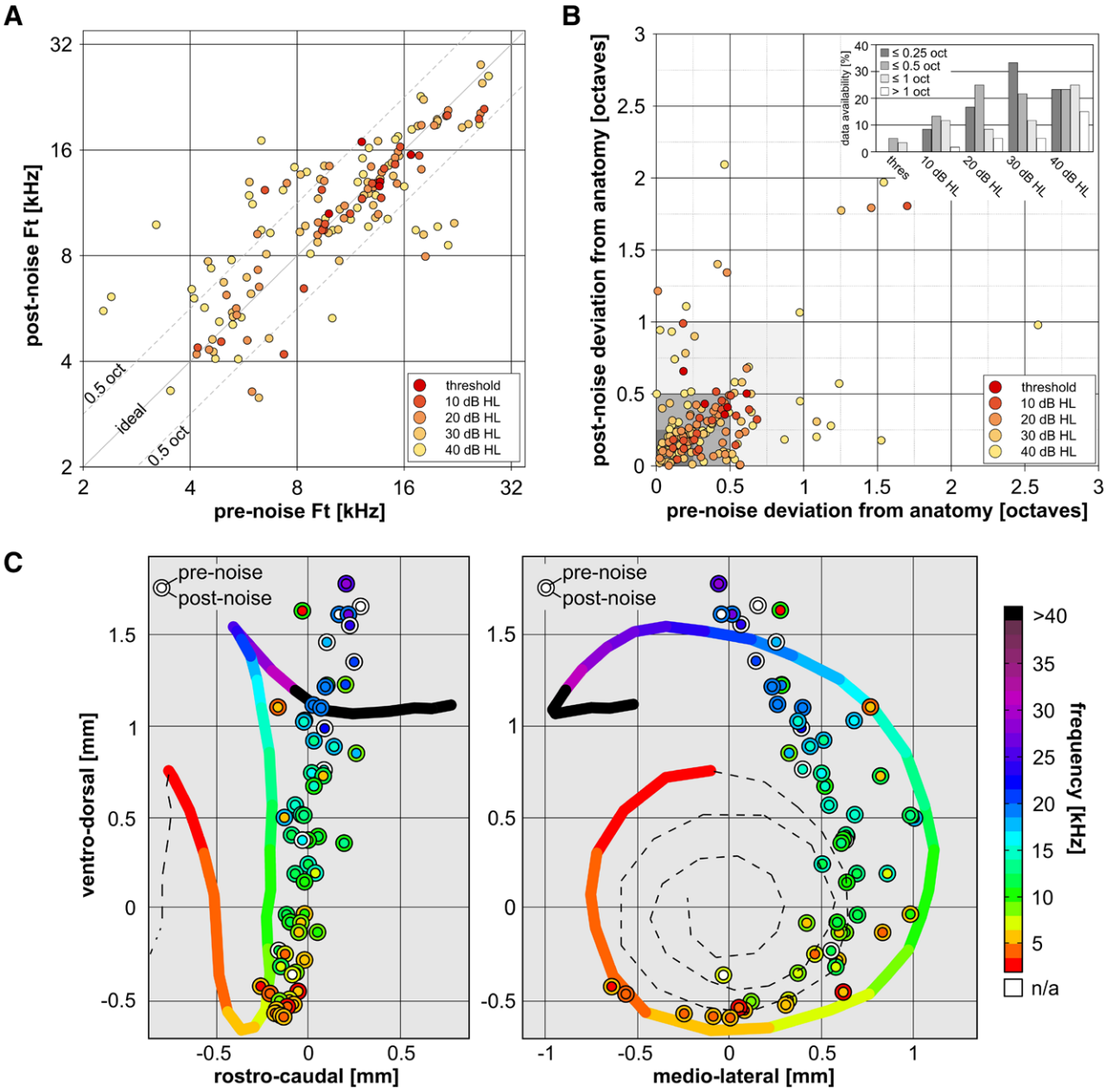


Fig. 5. The Ft remained stable after noise-exposure. A, Pre- and post-noise-exposure data correlated at sound levels between threshold and 40 dB HL. More than 75% of data points fall within ± 0.5 octaves from the ideal correlation (mean ± 0.37 | SD 0.29 oct). B, Both pre-noise-exposure and post-noise-exposure data correlate with the anatomical frequency estimates (Tsuji & Liberman 1997). A histogram of all data points and their difference between electrophysiologically determined and anatomically determined frequency positions is shown as an inset (see also comparison in Figure 2 in Supplemental Digital Content 1, http://links.lww.com/EANDH/B38). At a stimulation level of 30 dB HL the available percentage of Fts (pre-noise: 98%; post-noise: 72%) is high and their deviation from the anatomical frequency estimate (pre-noise: 0.32 ± 0.31 octaves; post-noise: 0.31 ± 0.35 octaves) is low (compare 40 dB HL pre | post data availability: 95% | 89%; deviation: 0.43 ± 0.47 oct. | 0.39 ± 0.43 oct.). C, The 30 dB HL data from panels (A) and (B) depicted as a combination of anatomically estimated, pre-noise-exposure, and post-noise-exposure frequency values in frontal and lateral 2D projections of the basal cochlear turn. The zero position serves as a reference point in the 2D projections. It was manually set to the center of the modiolus in the dorsoventral and mediolateral direction and near to the entry point of the internal meatus in the rostrocaudal direction (data points pre|post: A|B thr: n = 22|18; 10 dB HL: n = 47|26; 20 dB HL: 55/37; 30dB HL: 60|44; 40 dB HL: 58|54; C n = 61).

compared with 0.9 dB for controls. The difference was similar after noise exposure (outliers: 12.1 dB; controls 3.2 dB). In contrast, average lowest thresholds between 2 kHz and 32 kHz were within one SD of the global average (21.5 ± 9.9 dB SPL) after insertion (outliers: 26.7 dB SPL; controls: 16.7 dB SPL) and were comparable between both groups after noise exposure (global average: 26.9 ± 9.5 dB; outliers: 26.7 dB; controls 23.3 dB). In two of the three outliers, the Ft deviated more strongly from the anatomically estimated mid-point frequencies than the – equally deeply inserted – controls (Fig. 6C). Below 8 kHz the Ft was consistently lower than the anatomical estimate before noise exposure in both controls and outliers. After noise exposure, the Fts of all three outliers deviated more strongly from the anatomical estimate than any of the remaining cases (Fig. 6D).

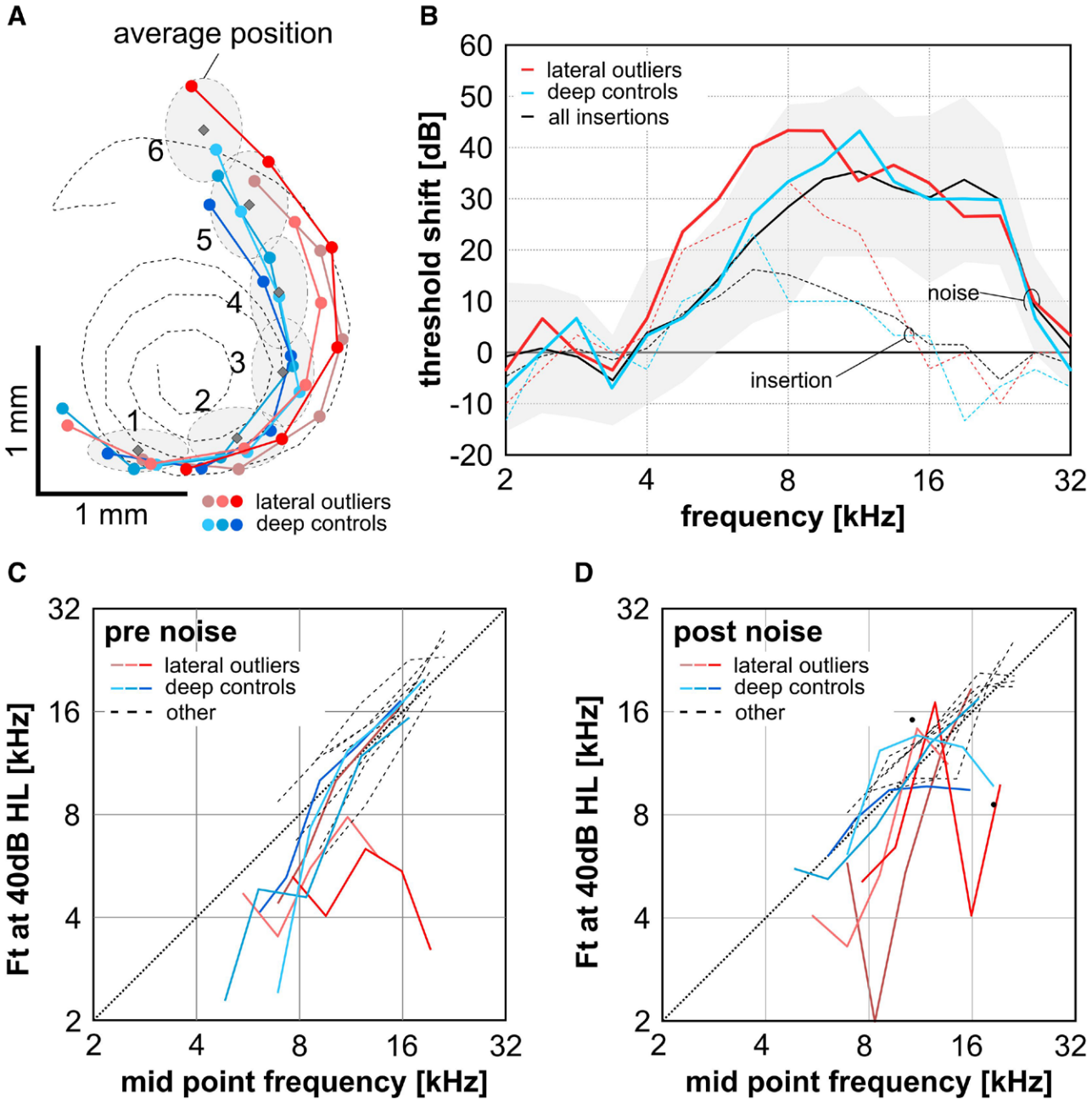


Fig. 6. A combination of electrophysiological measures and anatomically derived parameters can account for the deviations between the Fts and the anatomical midpoint frequencies in individual examples. A, The positions of three lateral CI positions ("outliers," red) are compared with three examples with similar insertion depths but more modiolar positions ("controls," blue) in a frontal 2D projection. The average positions of the 6 CI contacts in all 13 cases are shown as gray diamonds, the shaded ellipses refer to the SDs in the dorsoventral direction and mediolateral direction, respectively. B, A comparison of the threshold shift relative to the CAP audiogram before insertion (Fig. 3) reveals more damage 4.8 kHz and 13.5 kHz by the extreme insertions (dashed red line, average of 3; controls: dashed blue line, average of 3). Dashed black line represents the average of all 13 cases. C, Deviations of Ft from anatomically-determined electrode mid-point frequency before noise exposure. The cases are marked by the same color as in A and B. An apparent difference in the precision of Ft showed up between the extreme and control groups. Above 8 kHz the Fts of controls (blue lines) did not deviate more than the average of all insertions, but the outliers did (red lines). Two of the three outliers had large deviations between the anatomically estimated midpoint frequencies and the Fts before noise exposure. Below 8 kHz the deviation of the Ft from the midpoint frequency consistently resulted in an underestimation of the tonotopic position by the electrophysiological measure in both controls and outliers. D, After noise exposure, the difference between extreme and controls was still observable. (black dots: isolated data points)

This could be consistent with some additional damage caused by CI insertion. It is interesting to note that the three outliers in the data all stem from CI insertions that share similar features, distinguishing them from the rest of the insertions. This might account for some of the Ft variability in the dataset presented.

### Pooled Data Position Estimation

We subsequently pooled the data from all 61 recording positions of all animals and used them to predict changes in the Ft during CI advancement. Here the midpoint position of the individual CI contacts was used irrespective of which experiment it was derived from.

The normalized SP amplitudes (see Fig. 4B) at a stimulation sound level of 60 dB SPL were plotted against the relative distance of the recording position from the cochlear base before noise exposure (Fig. 7, for sound levels between 30 and 80 dB SPL, see Figure 3 in Supplemental Digital Content 1, http://links.lww.com/EANDH/B38). Individual plots were constructed for six different stimulation frequencies. The six frequencies were chosen to include the stimulation frequency with a tonotopic position apical of the most apical CI contact (i.e., 4 kHz) and the frequency with tonotopic position estimated basal of the most basal contact (i.e., 22.62 kHz). As a general pattern, the SP amplitudes were negative at recording positions basally to a given stimulation frequency and changed polarity close to the respective tonotopic position. This resulted in a frequency-dependent polarity inversion position analog to the position-dependent Ft. When the recording positions were remote from the excitation maximum, the SP amplitudes were small (10–20% distance at 4 kHz; 30–40% distance at 22.62 kHz) and reached their respective peak amplitude at about 10% distance from the turning position (compare 8 kHz stimulation for maximal trough amplitude at ~21% and 16 kHz stimulation for maximal peak amplitude at ~30%). Between these points the amplitudes decreased and the polarity reversed.

Based on these data we suggest the following procedure for implantation (see Fig. 7: 8 kHz): First the high-frequency border of the hearing range based on the individual subject's audiogram is determined. This defines the acoustic stimulation frequency. Bipolarly recorded SP to this stimulus when recorded basally to the corresponding tonotopic position will cause small, mostly negative SPs. Further insertion of the CI will lead to more negative SPs before further insertion will lead to a reversal of SPs polarity when the recording electrodes reach the active cochlear place.

After noise exposure, the general pattern of SP amplitudes over-insertion depths was still present despite a significant effect on hearing loss (Fig. 8). Despite differences we did not observe any significant difference between pre- and post noise- exposure Ft values (tested 2 kHz–32 kHz; paired two-tailed t-test, uncorrected $p = 0.76$, t-statistics = −0.30, Pearson's correlation r = 0.6; average difference: 0 ± 0.23 [normalized]). Trauma at the base (partially) compromised responses at positions basally from the 8 kHz target position (Fig. 8). Considering that the starting point for cochlear implantation in guinea pigs (16%

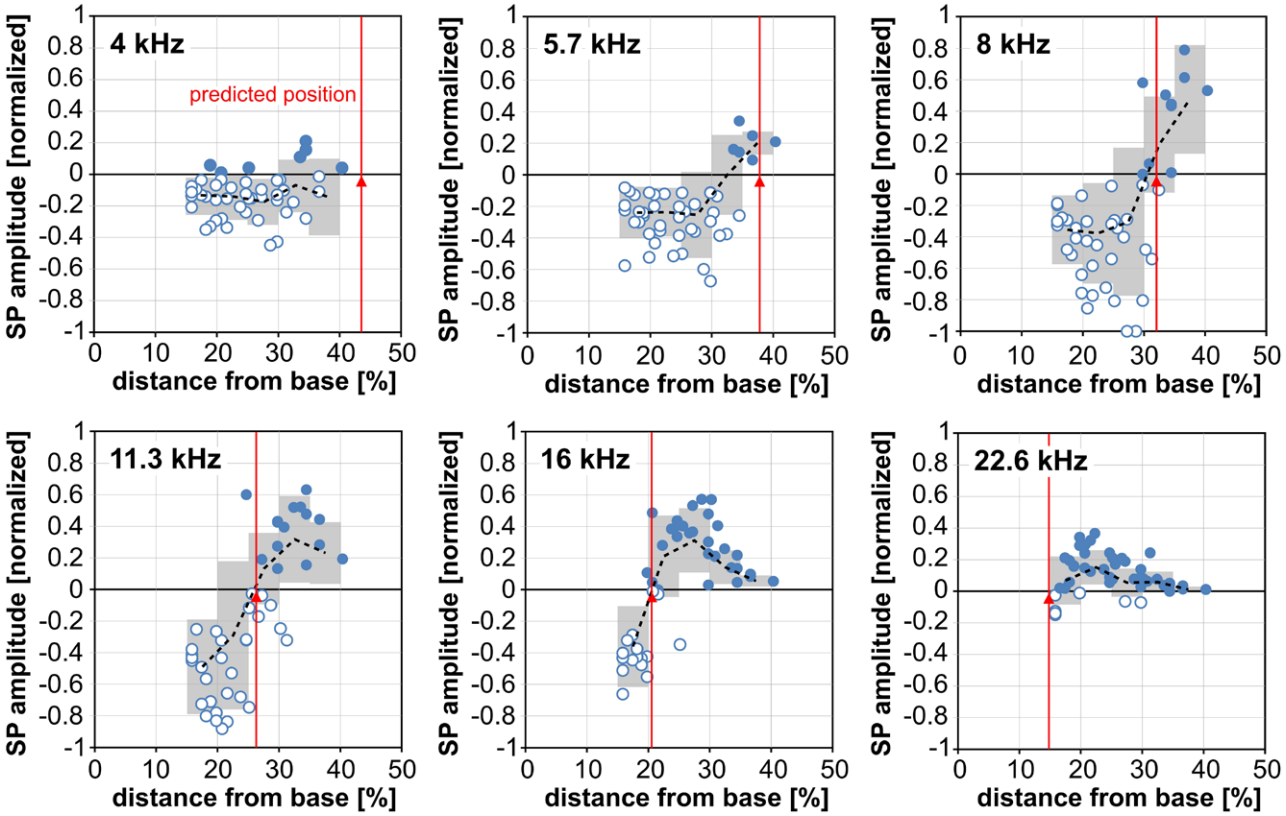


Fig. 7. Combining the recording data from all intracochlear recording positions from all implantations before noise exposure provided positional data between 16 and 40% distance from base (apex: 100% distance). These data allowed for the emulation of a hypothetical surgical approach, assuming a pure tone presented at a fixed frequency (insert at top of each panel) and a given sound level (60 dB SPL, data for 30 dB SPL – 80 dB SPL seen in Figure 3 in Supplemental Digital Content 1, http://links.lww.com/EANDH/B38). The frequency of the stimulus has an excitatory maximum at a given intracochlear depth (red marker, predicted from Tsuji & Liberman, 1997). The implant is hypothetically inserted toward the position of the maximum response. When the position of the CI was remote from the stimulation target, the SP amplitude was small and mostly negative. When the recording position approached the target, the SP amplitude first became more negative. Further approach to the target position made the SP again less negative. Passing the target position with the recording position led to an abrupt SP turning with positive amplitudes apical to the target. (Filed circles: positive SP amplitude, open circles: negative SP amplitude; red line: predicted position of stimulus frequency; solid black line: polynomial regression, regression coefficient shown in plots; dashed black line: average in 5% bins from 15 to 40% insertion; gray shading: SD for 5% bins, recording positions per panel: n = 61).

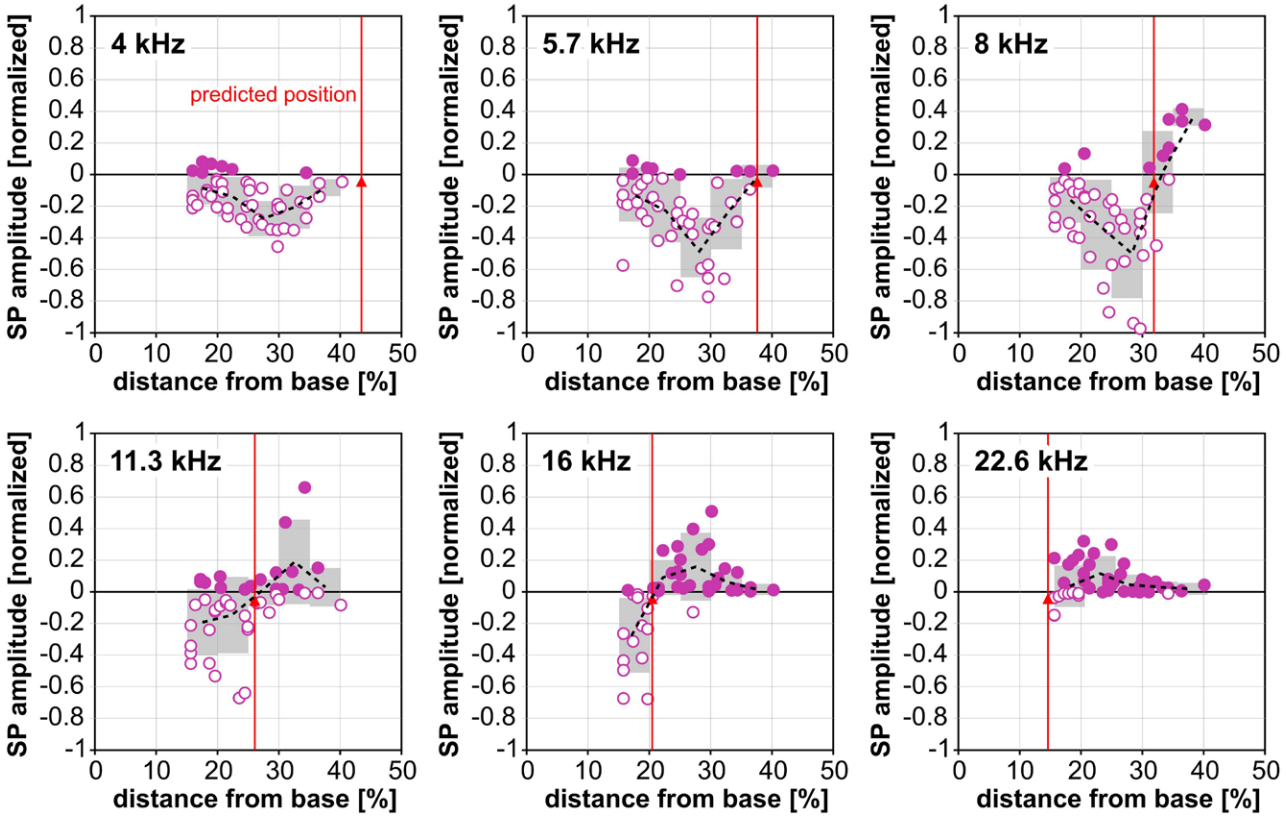


Fig. 8. Repeating the emulation of the CI insertion after noise exposure gave similar results as before noise exposure with SP turning at the target frequency. The overall reduced cochlear responsiveness at frequencies above 8 kHz (compare Fig. 3) led to a less pronounced SP response pattern at higher frequencies. This is especially apparent for a stimulation frequency of 11.31 kHz (compare Fig. 6B). (Filed circles: positive SP amplitude, open circles: negative SP amplitude; Red line: predicted tonotopic mid-point position of stimulus; dashed black line: average in 5% bins from 15 to 40% insertion; gray shading: SD for 5% bins).

insertion depth) is far basal from the 8 kHz target position, the recorded SP values allow an estimation of the approach to the target: values first decrease during insertion to subsequently increase again upon approaching the region corresponding to the stimulus frequency. A polarity reversal finally signifies that the implant has reached the tonotopic place of the stimulus.

### Minimum Tracking as Simplified SP Monitoring Application

The results suggest that polarity-change in SPs recorded bipolarly will serve as a marker of intracochlear electrode position. In a clinical setting with only limited low-frequency hearing preserved, however, it may often not be feasible to insert the CI deep enough to see the SP polarity reversal. On the basis of the Ft prediction presented above, we suggest minimum tracking as a potentially feasible clinical approach (Fig. 9). In this approach, a series of intracochlear recordings along the insertion path would allow limiting the insertion to that portion of the cochlea that generates negative SP polarity. During advancement of the CI, the SP amplitude recorded at each position would be compared with the previously-recorded one. If the SP amplitude stopped becoming more negative despite advancement of the electrode over a critical distance, it would indicate a close approach to the Ft position. In such case the CI insertion would be terminated.

A suitable critical distance criterion would be 5% cochlear length. This suggestion is based on the observation that the distance between the SP minimum, basally to the turning point, and the maximum, apically to the turning point, amounted to approximately 10% of cochlear length.

The minimum-tracking method gave good results when applied to post noise-exposure Ft predictions (data from Fig. 8) with well discernible turning point (8 kHz stimulation) and with less clear data (11.3 kHz stimulation). In both exemplary cases, the presumed endpoint of insertion would have been close to the anatomically estimated midpoint (8 kHz: 2.5%; 11.3 kHz: 3%) as well as the turning point of the pooled data (8 kHz: ~1%; 11.3 kHz: ~2%).

## DISCUSSION

The aim of the present study was to obtain a reliable marker of positional information for the contact of the CI using intracochlear ECochG. The data demonstrate that bipolar recording of SP can assess the cochlear recording position using the polarity reversal of SP: negative SPs were recorded basally from the excited cochlear partition and positive SPs were recorded apically to it. The acoustic stimulation frequency at which the polarity reversed at a given recording position (Ft) provided reliable information on the cochlear position of the recording contacts within ±0.37 octaves (SD 0.29 octaves). Approximately 70% of the variability of Ft was due to cochleotopic position of the recording electrode. Some of the remaining variability could be associated with lateral electrode position. We suggest a minimum-tracking approach that illustrates a potential clinical

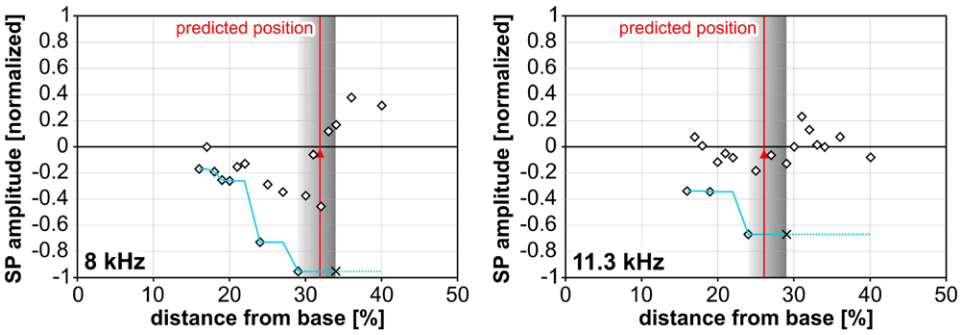


Fig. 9. A potential approach for the clinical use of the SP would be a minimum-tracking method, exemplified above for two frequency examples. The post-noise-exposure data from Figure 8 for 8 kHz and 11.3 kHz (both at 60 dB SPL) were condensed to discrete data points by assigning the median SP amplitude to each distance with more than one amplitude value. In case of data with high SP amplitude fluctuations, the tracking of the overall minimum amplitude throughout insertion might serve to approximate the Ft-position without inserting far beyond that point. During insertion, the overall minimum amplitude (blue line) is calculated from all recorded SP amplitudes (open diamonds) recorded over the previous positions. Insertion was halted (black "x") when the minimum would not change over a pre-defined insertion range (here: 5% cochlear length based on the common distance between SP amplitude minimum and maximum). In the Ft predictions shown here, this simplified approach would have led to an insertion stop within 1 to 2% cochlear distance of the pooled turning point (8 kHz: ~33%; 11.3 kHz: ~27%) and 2.5 to 3% from the anatomical mid-point estimate (8 kHz: ~32%; 11.3 kHz: ~26%).

approach to utilizing bipolar intracochlear SP recordings to gain information on the CI electrode position relative to a predefined frequency or frequency range.

## Methodological Limitations

The frequency range investigated in this study was adjusted to the hearing range of the animal model and the cochlear partition accessible to a CI insertion in the guinea pig cochlea, which differs from a typical CI subject. We hypothesize that the principles underlying the presented results are the same for lower frequencies in human subjects, given the presence of recordable SPs.

Hearing thresholds of the animals after cochleostomy (Fig. 3) were well comparable to normal hearing albino and pigmented guinea pigs (ABR: Huetz et al. 2014; CAP: Conlee et al. 1989; Behavior: Heffner et al. 1971). This demonstrates that cochlear implantation is possible without significant cochlear trauma.

Helmstaedter et al. (2018) showed that in normal-hearing guinea pigs the amplitude of SP in response to a range of frequencies and intensities is correlated with the intracochlear position of the CI electrode in monopolar recordings. While CMs could also convey some positional information, CM-derived position information was not reliable in Helmstaedter et al. CMs and CAPs could rather serve as markers for the physiological state of the cochlea (or cochlear health). In fact, CMs have previously been successfully used as a marker of cochlear trauma during cochlear implantation (Adunka et al. 2010; Adunka et al. 2016; Giardina et al. 2019).

With the bipolar recording configuration used in the present study, the Ft were much better discernible than in the previous study (Helmstaedter et al. 2018). In the present results, the position-dependent polarity reversal of the SP (Ft) was present from threshold to levels up to 80 dB SPL. We did observe a shift of Fts to lower frequencies with increasing sound levels (Fig. 4C). The shift was moderate (0.30 ± 0.30 octaves) and corresponded to an expected downward shift in the cochlear excitation with increasing sound level (Johnstone et al. 1986; Ruggero et al. 1997), further supporting the usefulness of the method.

While hearing impairment led to reduced SP amplitudes, discernible SPs still provided positional information similar to cochleae without damage. This suggests that moderate hearing loss (Fig. 3) did not significantly bias the outcome of the method. In fact, the sound level of 60 dB SPL may not have been sufficient for supra-threshold stimulation above 8 kHz after noise exposure (compare Fig. 3). This further corresponds to the clinical situation with high-frequency hearing loss. Indeed, clinical studies show that responses to an acoustic stimulus are absent at the base and present at the apex (Lenarz 2017; Dazert et al. 2020). Nonetheless, the impact of more extensive hearing loss remains to be studied in the future.

The validation of the present results showed a precision of the positional information within ±0.37 octaves, corresponding to approximately 0.95 mm in the guinea pig cochlea (Greenwood 1990). Given that the recording contacts of the animal CI have a spacing of 0.7 mm, this is in the range of the measuring points along the cochlea. Thus the positional precision of the method corresponds to the spacing of the measurement contacts. Using an implant with narrower spacing of contacts would likely increase the precision.

Due to the restricted implantation depths (~270°) and the hearing range of the guinea pig, we could not determine how well the SP would be suited as position marker for frequencies below 1 kHz, where human EAS candidates typically show residual hearing. Furthermore, in the present study, we used CIs placed at a constant location and responses were recorded with different electrode contacts along with the array. In the clinical condition, the implant will be advanced and the measurement will be performed by the same (apical) electrode contacts. We decided on the present method so that we can validate the results and assess their precision using µCT performed after the recordings were completed. The two approaches further differ in the biasing factor of the displaced volume of the perilymph - which was constant in the present experiments but will increase with advancing implantation in the clinical setting. Therefore a follow-up clinical study (already initiated at our clinics) will have to provide insights into the effect of these factors.

## Physiological Interpretation

The present study observed only limited implantation trauma, comparable to the results of previous studies from

our laboratory with shorter CIs (Sato et al. 2016). Elevation of CAP thresholds between 5.7 kHz and 9.5 kHz with full insertion of CI shows that deep insertion of CI can affect the hearing. This has been shown in a separate study using the insertion data from cases further analyzed in the present study (Andrade et al. 2020). It is interesting that this threshold elevation was not observed along the whole length of the electrode, but was rather limited to frequencies below 11.3 kHz. While the insertion of the implant led to a threshold deterioration at frequencies below 11.3 kHz, it was less pronounced than in a previous study (Helmstaedter et al. 2018). A separate analysis of four cases in which only five contacts were inserted revealed better hearing protection with near-normal thresholds, comparable to post-insertion IC thresholds reported in Sato et al. (2016) using shorter CIs. This demonstrates that implantation up to the point of perceptible resistance, as often is in clinical practice, may lead to cochlear trauma (Andrade et al. 2020). The present study additionally introduced hearing impairment by exposure to band-pass noise. Noise exposure with a noise band at either 8 kHz to 12 kHz (N = 10) or 14 kHz to 18 kHz (N = 8) resulted in significant threshold elevation at frequencies slightly higher than the noise. Threshold shifts in frequencies higher than the applied acoustic stimulus have been similarly described before and are known to be caused by cochlear nonlinearities (Cody & Johnstone 1981; Puel et al. 1998; Robles & Ruggero 2001). Taken together, the data thus demonstrate the expected effects of high-level bandpass noise on hearing thresholds and, with careful cochlear implantation, a limited implantation trauma.

**SP as a Marker of CI Position**

We used SPs as markers of intracochlear position. SPs originate mainly from hair cells (Dallos 1973; Johnstone & Johnstone 1966; Forgues et al. 2014; Pappa et al. 2019) and thus may provide positional information in the cochlea for pure-tone stimulation. We found that the tonotopic intracochlear recording position is marked by a polarity reversal of the SP in bipolar recordings at stimulation frequency defined as turning frequency or Ft. The individual contributions of outer and inner hair cells and neural components to SPs have not been fully resolved yet (Pappa et al. 2019). The SP amplitude depends on the preservation of both inner and outer hair cells (Durrant et al. 1998); however, it remains unclear how many hair cells have to be preserved to generate a recordable SP. Here we used band-filtered noise at a level of 110 dB SPL for 30 minutes to induce a high-frequency noise trauma. The subsequent threshold shift was likely caused by both excitotoxic synaptic damage and damage to outer hair cells, while keeping inner hair cells largely intact (Puel et al. 1998). Thus the stability of the SP polarity reversal after noise exposure (pre/post deviation: ± 0.37 octaves | SD 0.29 oct) might be due to the preserved hair cell function. It is interesting that sometimes even in deaf subjects electrocochleographic signals can be recorded (Tejani et al. 2021). Such findings could result from hair cells that are not contacted by the primary afferents.

The method presented here tends to result in Fts basal to the actual intracochlear frequency position (Figs. 7 and 8), especially for low stimulation frequencies and high SPLs (See Figure 3 in Supplemental Digital Content 1, http://links.lww.com/EANDH/B38). This could be a consequence of the heterogenous contribution of IHCs and OHCs to the SP (Cody & Russell 1987). The precision of the recordings could be improved, for example, by reducing the distance between the recording electrodes or by using an adjusted SP response function that balances such an effect.

At low frequencies, the SP is thought to comprise an asymmetry in CM positive and negative excursion (Cody & Russell 1985). SPs were also recorded in humans for frequencies below 1 kHz (Ferraro et al. 1994; Ferraro 2010; Riggs et al. 2017; Pappa et al. 2019; Dalbert et al. 2020; Eyvazi et al. 2020). Therefore, we think that bipolar, intracochlear ECochG recordings of the SP during CI surgery could be a promising approach to localize the recording contact relative to the stimulated portion of the cochlea even in subjects with only low-frequency hearing. A complicating factor in the clinical setting is the recording equipment because often the signal conditioning (particularly the filter settings) is not specified and some level of high-pass filtering is involved in commercial systems to stabilize the recording. However, when SP can be recorded, the present study demonstrates that it provides precise information on the position of the recording electrodes. Human CIs usually have contact spacings wider than the 0.7 mm of the animal implant used in this study (e.g., 2.1 mm spacing in a MED-EL Flex28). In such case adding one more narrowly spaced contact pair at the implant tip would enable bipolar monitoring of the SP with improved precision.

The position of the electrode was assessed using polarity reversal of SP. Large differences in bipolar-recorded signals (shown by polarity reversals) correspond to places with non-zero second derivatives over location and thus places with high-current source densities (Ranck 1975; Rattay 1987). These further correspond to the location where charges enter or exit the perilymph. Indeed, the Ft correlated well with positions corresponding to the frequency representation of the given stimulus, projected on the μCT scans using the Greenwood function modified for the guinea pig (Tsuji & Liberman 1997). Such validation was also successful in hearing-impaired cochleae (with hearing loss up to ~40 dB). The precision of the SP-estimated cochlear place was high (mean: 0.95 mm), given the size and distance of the recording contacts (see Materials and Methods). It is interesting that a downward shift of the turning frequency was observed with increasing level – an observation well corresponding to the downward shift of the most exciting cochlear region with increasing stimulus level (Johnstone et al. 1986; Ruggero et al. 1997). Thus, all the properties of the recorded signals meet physiological expectations. Variation of cochlear place contributed to ~70% of the variability of Ft. This value is high for biological signals. The modiolar-abmodiolar location of the implant (Fig. 5) likely contributed to the remaining variability. The relative rigidity of the animal CI due to narrow contact spacing might have contributed to trauma during insertion along the lateral wall. Local immobilization of the BM by a laterally inserted CI (Kiefer et al. 2006) could have contributed to the hearing loss (Fig. 6). Human atraumatic lateral-wall-electrodes are longer, the spacing between contacts is larger and the resulting total flexibility is higher than in the present animal CIs. Thus, the effects observed as "outliers" in the present data, related to the lateral electrode position, will likely be different in the human lateral wall electrodes. Overall; however, the results illustrate the applicability of the suggested method to determine the intracochlear contact position.

Moderate hearing loss did not reduce the precision of our method. The stimulation level relative to the auditory threshold mainly impacted the data availability, that is, close to the threshold, SPs could not always be recorded, yet where obtained, the recorded data carried a high degree of positional information (Fig. 5A, B). The lack of extreme deviations from the anatomical estimate close to auditory threshold is likely due to a more localized excitation at the organ of the Corti close to the threshold. At higher SPL the SPs could be more reliably recorded, and the precision of Ft was sufficient for the present purposes, even though the spread of the data slightly increased. For clinical translation, the positional precision is likely highest close to threshold levels, but the signal yield was highest at 30 dB above the hearing threshold, where the methods still provided reliable positional estimates. However, slight intensity-dependent shifts of the most excited cochlear position need to be taken into account. A variation of acoustic chirps (Elberling et al. 2007; Adel et al. 2020) could further increase SP amplitudes and the signal yield and thus improve the outcomes in hearing-impaired individuals.

### Clinical Relevance

Here we used multiple stimulation frequencies and SPLs to identify the recording electrode position within the cochlea. This approach is time-consuming and therefore not feasible in a clinical setting. The pooled Ft data (Figs. 7–9) demonstrate that stimulating at a fixed frequency and SPL will also provide reliable positional information. Here we suggest a minimum-tracking method that might be applicable in a clinical setting (Fig. 9). In the pre-operative examination, the frequency of the high-frequency border of residual hearing (based on the patient's audiogram) will define the stimulation frequency. A frequency or frequency band of this range will subsequently be used for acoustic stimulation during CI insertion. Increasingly negative amplitudes of the SP before the polarity reversal in a bipolar configuration will indicate an approach to the stimulation frequency region. This approach is less time-consuming and prevents an intrusion of the apical electrode into the intact part of the cochlea. We added a flowchart of the proposed clinical approach Figure 4 in Supplemental Digital Content 1, http://links.lww.com/EANDH/B38. While it remains to be studied how well this minimum-tracking would work on actual insertion data with usually small SPs, the present results illustrate that it has translational potential.

## CONCLUSIONS

The present study provides evidence that SPs represent a reliable marker for the intracochlear position of the recording electrodes. Using bipolar recording configuration, SP polarity reversals identify the cochlear position well. We suggest a potential minimum-tracking method to make use of the positional information gained from the SP during CI implantation.

## ACKNOWLEDGMENTS

This study was partially funded by Deutsche Forschungsgemeinschaft (DFG Exc 2271, Cluster of Excellence "Hearing4All"). The research cochlear implants were provided by MedEl Comp. (Innsbruck). There are no conflicts of interest, financial, or otherwise.

The authors would like to thank Karl-Jürgen Kühne for preparing the μCT scans. The authors also thank Felix P. Aplin for proofreading the final manuscript. The authors thank MedEl (Innsbruck) for providing the research CIs. This work was supported by Deutsche Forschungsgemeinschaft (DFG Exc 2271, Cluster of Excellence "Hearing4All").

P.B. designed and supervised the experiments, analyzed the data and drafted the manuscript, L.R. analyzed the data and edited the manuscript, J.A. performed the experiments and edited the manuscript, T.L. designed the study and obtained the funding, A.K. designed the study, obtained the funding and edited the manuscript. All authors approved the final version of the manuscript.

Address for correspondence: Peter Baumhoff, Department of Experimental Otology, ENT Clinics, Hannover Medical School, Stadtfelddamm 34, 30625 Hannover, Germany. E-Mail: baumhoff.peter@mh-hannover.de

Received August 12, 2021; accepted May 23, 2022; published online ahead of print July 27, 2022.

## REFERENCES

Adel, Y., Tillein, J., Petzold, H., Weissgerber, T., & Baumann, U. (2021). Band-limited chirp-evoked compound action potential in guinea pig. *Ear Hear*, *42*, 142–162.

Adunka, O. F., Giardina, C. K., Formeister, E. J., Choudhury, B., Buchman, C. A., Fitzpatrick, D. C. (2016). Round window electrocochleography before and after cochlear implant electrode insertion. *Laryngoscope, 126*, 1193–1200.

Adunka, O. F., Mlot, S., Suberman, T. A., Campbell, A. P., Surowitz, J., Buchman, C. A., Fitzpatrick, D. C. (2010). Intracochlear recordings of electrophysiological parameters indicating cochlear damage. *Otol Neurotol, 31*, 1233–1241.

de Andrade, J. S. C., Baumhoff, P., Cruz, O. L. M., Lenarz, T., Kral, A. (2020). Cochlear implantation in an animal model documents cochlear damage at the tip of the implant. *Braz J Otorhinolaryngol, 88,* 546–555.

Bester, C., Razmovski, T., Collins, A., Mejia, O., Foghsgaard, S., Mitchell-Innes, A., Shaul, C., Campbell, L., Eastwood, H., O'Leary, S. (2020). Four-point impedance as a biomarker for bleeding during cochlear implantation. *Sci Rep, 10*, 2777.

Brown, D. J., & Patuzzi, R. B. (2010). Evidence that the compound action potential (CAP) from the auditory nerve is a stationary potential generated across dura mater. *Hear Res, 267*, 12–26.

Campbell, L., Kaicer, A., Sly, D., Iseli, C., Wei, B., Briggs, R., O'Leary, S. (2016). Intraoperative real-time cochlear response telemetry predicts hearing preservation in cochlear implantation. *Otol Neurotol, 37*, 332–338.

Canfarotta, M. W., O'Connell, B. P., Giardina, C. K., Buss, E., Brown, K. D., Dillon, M. T., Rooth, M. A., Pillsbury, H. C., Buchman, C. A., Adunka, O. F., Fitzpatrick, D. C. (2021). Relationship between electrocochleography, angular insertion depth, and cochlear implant speech perception outcomes. *Ear Hear, 42*, 941–948.

Cheatham, M. A., & Dallos, P. (1984). Summating potential (SP) tuning curves. *Hear Res, 16*, 189–200.

Cody, A. R., & Johnstone, B. M. (1981). Acoustic trauma: Single neuron basis for the "half-octave shift". *J Acoust Soc Am, 70*, 707–711.

Cody, A. R., & Russell, I. J. (1985). Outer hair cells in the mammalian cochlea and noise-induced hearing loss. *Nature, 315*, 662–665.

Cody, A. R., & Russell, I. J. (1987). The response of hair cells in the basal turn of the guinea-pig cochlea to tones. *J Physiol, 383*, 551–569.

Conlee, J. W., Gill, S. S., McCandless, P. T., Creel, D. J. (1989). Differential susceptibility to gentamicin ototoxicity between albino and pigmented guinea pigs. *Hear Res, 41*, 43–51.

Dalbert, A., Huber, A., Veraguth, D., Roosli, C., Pfiffner, F. (2016). Assessment of cochlear trauma during cochlear implantation using electrocochleography and cone beam computed tomography. *Otol Neurotol, 37*, 446–453.

Dalbert, A., Pfiffner, F., Röösli, C., Thoele, K., Sim, J. H., Gerig, R., Huber, A. M. (2015). Extra- and intracochlear electrocochleography in cochlear implant recipients. *Audiol Neurootol, 20*, 339–348.

Dalbert, A., Rohner, P., Roosli, C., Veraguth, D., Huber, A., Pfiffner, F. (2020). Correlation between electrocochleographic changes during surgery and hearing outcome in cochlear implant recipients: A case report and systematic review of the literature. *Otol Neurotol, 41*, 318–326.

Dalbert, A., Sijgers, L., Grosse, J., Veraguth, D., Roosli, C., Huber, A., Pfiffner, F. (2021). Simultaneous intra- and extracochlear

electrocochleography during electrode insertion. *Ear Hear, 42*, 414–424.
Dallos, P. (1973). In P. Dallos (Ed.), *The Auditory Periphery - Biophysics and Physiology* (1st ed.). Academic Press.
Dazert, S., Thomas, J. P., Loth, A., Zahnert, T., Stöver, T. (2020). Cochlear implantation. *Dtsch Arztebl Int, 117*, 690–700.
Dhanasingh, A., & Hochmair, I. (2021). Special electrodes for demanding cochlear conditions. *Acta Otolaryngol, 141*(Sup1), 157–177.
Downing, M. (2018). Electrode designs for protection of the delicate cochlear structures. *J Int Adv Otol, 14*, 401–403.
Driscoll, V. D., Welhaven, A. E., Gfeller, K., Oleson, J., Olszewski, C. P. (2016). Music perception of adolescents using electroacoustic hearing. *Otol Neurotol, 37*, e141–e147.
Durrant, J. D., Wang, J., Ding, D. L., Salvi, R. J. (1998). Are inner or outer hair cells the source of summating potentials recorded from the round window? *J Acoust Soc Am, 104*, 370–377.
Eggermont, J. J. (1976). Analysis of compound action potential responses to tone bursts in the human and guinea pig cochlea. *J Acoust Soc Am, 60*, 1132–1139.
Eggermont, J. J. (2017). Effects of long-term non-traumatic noise exposure on the adult central auditory system. Hearing problems without hearing loss. *Hear Res, 352*, 12–22.
Elberling, C., Don, M., Cebulla, M., Stürzebecher, E. (2007). Auditory steady-state responses to chirp stimuli based on cochlear traveling wave delay. *J Acoust Soc Am, 122*, 2772–2785.
van Emst, M. G., Klis, S. F., Smoorenburg, G. F. (1995). Tetraethylammonium effects on cochlear potentials in the guinea pig. *Hear Res, 88*, 27–35.
Eyvazi, M., Pourbakht, A., Sameni, S. J., Kamali, M. (2020). Clinical evaluation of a new electrocochleography recording electrode. *Auditory and Vestibular Research, 29*, 93–100.
Ferraro, J. A. (2010). Electrocochleography: A review of recording approaches, clinical applications, and new findings in adults and children. *J Am Acad Audiol, 21*, 145–152.
Ferraro, J. A., Thedinger, B. S., Mediavilla, S. J., Blackwell, W. L. (1994). Human summating potential to tone bursts: observations on tympanic membrane versus promontory recordings in the same patients. *J Am Acad Audiol, 5*, 24–29.
Forgues, M., Koehn, H. A., Dunnon, A. K., Pulver, S. H., Buchman, C. A., Adunka, O. F., Fitzpatrick, D. C. (2014). Distinguishing hair cell from neural potentials recorded at the round window. *J Neurophysiol, 111*, 580–593.
Giardina, C. K., Brown, K. D., Adunka, O. F., Buchman, C. A., Hutson, K. A., Pillsbury, H. C., Fitzpatrick, D. C. (2019). Intracochlear electrocochleography: Response patterns during cochlear implantation and hearing preservation. *Ear Hear, 40*, 833–848.
Greenwood, D. D. (1990). A cochlear frequency-position function for several species–29 years later. *J Acoust Soc Am, 87*, 2592–2605.
Harris, M. S., Riggs, W. J., Koka, K., Litvak, L. M., Malhotra, P., Moberly, A. C., O'Connell, B. P., Holder, J., Di Lella, F. A., Boccio, C. M., Wanna, G. B., Labadie, R. F., Adunka, O. F. (2017). Real-time intracochlear electrocochleography obtained directly through a cochlear implant. *Otol Neurotol, 38*, e107–e113.
Haumann, S., Imsiecke, M., Bauernfeind, G., Büchner, A., Helmstaedter, V., Lenarz, T., Salcher, R. B. (2019). Monitoring of the inner ear function during and after cochlear implant insertion using electrocochleography. *Trends Hear, 23*, 2331216519833567.
Heffner, R., Heffner, H., Masterton, B. (1971). Behavioral measurements of absolute and frequency-difference thresholds in guinea pig. *J Acoust Soc Am, 49*, 1888–1895.
Helmstaedter, V., Lenarz, T., Erfurt, P., Kral, A., Baumhoff, P. (2018). The summating potential is a reliable marker of electrode position in electrocochleography: Cochlear implant as a theragnostic probe. *Ear Hear, 39*, 687–700.
Huetz, C., Guedin, M., Edeline, J. M. (2014). Neural correlates of moderate hearing loss: Time course of response changes in the primary auditory cortex of awake guinea-pigs. *Front Syst Neurosci, 8*, 65.
von Ilberg, C. A., Baumann, U., Kiefer, J., Tillein, J., Adunka, O. F. (2011). Electric-acoustic stimulation of the auditory system: A review of the first decade. *Audiol Neurootol, 16* Suppl 2, 1–30.
Imsiecke, M., Krüger, B., Büchner, A., Lenarz, T., Nogueira, W. (2020). Interaction between electric and acoustic stimulation influences speech perception in ipsilateral EAS users. *Ear Hear, 41*, 868–882.
Iso-Mustajärvi, M., Sipari, S., Löppönen, H., Dietz, A. (2020). Preservation of residual hearing after cochlear implant surgery with slim modiolar electrode. *Eur Arch Otorhinolaryngol, 277*, 367–375.
Johnstone, B. M., Patuzzi, R., Yates, G. K. (1986). Basilar membrane measurements and the travelling wave. *Hear Res, 22*, 147–153.
Johnstone, J. R., & Johnstone, B. M. (1966). Origin of summating potential. *J Acoust Soc Am, 40*, 1405–1413.
Kamerer, A. M., Diaz, F. J., Peppi, M., Chertoff, M. E. (2016). The potential use of low-frequency tones to locate regions of outer hair cell loss. *Hear Res, 342*, 39–47.
Kiefer, J., Böhnke, F., Adunka, O., Arnold, W. (2006). Representation of acoustic signals in the human cochlea in presence of a cochlear implant electrode. *Hear Res, 221*, 36–43.
Koka, K., Riggs, W. J., Dwyer, R., Holder, J. T., Noble, J. H., Dawant, B. M., Ortmann, A., Valenzuela, C. V., Mattingly, J. K., Harris, M. M., O'Connell, B. P., Litvak, L. M., Adunka, O. F., Buchman, C. A., Labadie, R. F. (2018). Intra-cochlear electrocochleography during cochear implant electrode insertion is predictive of final scalar location. *Otol Neurotol, 39*, e654–e659.
Krüger, B., Büchner, A., Nogueira, W. (2017). Simultaneous masking between electric and acoustic stimulation in cochlear implant users with residual low-frequency hearing. *Hear Res, 353*, 185–196.
Lenarz, T. (2017). Cochlear implant – state of the art. *Laryngo-Rhino-Otologie*, *96*, S123–S151.
Lenarz, T., Timm, M. E., Salcher, R., Prenzler, N., Lesinski-Schiedat, A., Büchner, A. (2020). Das Konzept der individuellen partiellen Cochlea Implantation für Patienten mit nutzbarem Restgehör. *Laryngo-Rhino-Otologie, 99*(S 02). doi: 10.1055/s-0040-1711750
Lenarz, T., Timm, M. E., Salcher, R., Büchner, A. (2019). Individual hearing preservation cochlear implantation using the concept of partial insertion. *Otol Neurotol, 40*, e326–e335.
Lorens, A., Walkowiak, A., Polak, M., Kowalczuk, A., Furmanek, M., Skarzynski, H., Obrycka, A. (2019). Cochlear microphonics in hearing preservation cochlear implantees. *J Int Adv Otol, 15*, 345–351.
Mandalà, M., Colletti, L., Tonoli, G., Colletti, V. (2012). Electrocochleography during cochlear implantation for hearing preservation. *Otolaryngol Head Neck Surg, 146*, 774–781.
Miranda, P. C., Sampaio, A. L., Lopes, R. A., Ramos Venosa, A., de Oliveira, C. A. (2014). Hearing preservation in cochlear implant surgery. *Int J Otolaryngol, 2014*, 468515.
Nagy, R., Jarabin, J. A., Perényi, Á., Dimák, B., Tóth, F., Jóri, J., Kiss, J. G. Rovó, L. (2018). Long-term hearing preservation with slim perimodiolar CI532® cochlear implant array. *Am J Otolaryngol, 1*, Azonosító-1019.
O'Connell, B. P., Cakir, A., Hunter, J. B., Francis, D. O., Noble, J. H., Labadie, R. F., Zuniga, G., Dawant, B. M., Rivas, A., Wanna, G. B. (2016). Electrode location and angular insertion depth are predictors of audiologic outcomes in cochlear implantation. *Otol Neurotol, 37*, 1016–1023.
O'Connell, B. P., Hunter, J. B., Haynes, D. S., Holder, J. T., Dedmon, M. M., Noble, J. H., Dawant, B. M., Wanna, G. B. (2017). Insertion depth impacts speech perception and hearing preservation for lateral wall electrodes. *Laryngoscope, 127*, 2352–2357.
Pappa, A. K., Hutson, K. A., Scott, W. C., Wilson, J. D., Fox, K. E., Masood, M. M., Giardina, C. K., Pulver, S. H., Grana, G. D., Askew, C., Fitzpatrick, D. C. (2019). Hair cell and neural contributions to the cochlear summating potential. *J Neurophysiol, 121*, 2163–2180.
Pietsch, M., Aguirre Dávila, L., Erfurt, P., Avci, E., Lenarz, T., Kral, A. (2017). Spiral form of the human cochlea results from spatial constraints. *Sci Rep, 7*, 7500.
Pillsbury, H. C. 3rd, Dillon, M. T., Buchman, C. A., Staecker, H., Prentiss, S. M., Ruckenstein, M. J., Bigelow, D. C., Telischi, F. F., Martinez, D. M., Runge, C. L., Friedland, D. R., Blevins, N. H., Larky, J. B., Alexiades, G., Kaylie, D. M., Roland, P. S., Miyamoto, R. T., Backous, D. D., Warren, F. M., El-Kashlan, H. K., et al. (2018). Multicenter US clinical trial with an Electric-Acoustic Stimulation (EAS) system in adults: Final outcomes. *Otol Neurotol, 39*, 299–305.
Puel, J. L., Ruel, J., Gervais d'Aldin, C., Pujol, R. (1998). Excitotoxicity and repair of cochlear synapses after noise-trauma induced hearing loss. *Neuroreport, 9*, 2109–2114.
Ranck, J. B. Jr. (1975). Which elements are excited in electrical stimulation of mammalian central nervous system: A review. *Brain Res, 98*, 417–440.

Rattay, F. (1987). Ways to approximate current-distance relations for electrically stimulated fibers. *J Theor Biol, 125*, 339–349.

Reiss, L. A. (2020). Cochlear implants and other inner ear prostheses: Today and tomorrow. *Curr Opin Physiol, 18*, 49–55.

Riggs, W. J., Roche, J. P., Giardina, C. K., Harris, M. S., Bastian, Z. J., Fontenot, T. E., Buchman, C. A., Brown, K. D., Adunka, O. F., Fitzpatrick, D. C. (2017). Intraoperative electrocochleographic characteristics of auditory neuropathy spectrum disorder in cochlear implant subjects. *Front Neurosci, 11*, 416.

Robles, L., & Ruggero, M. A. (2001). Mechanics of the mammalian cochlea. *Physiol Rev, 81*, 1305–1352.

Ruggero, M. A., Rich, N. C., Recio, A., Narayan, S. S., Robles, L. (1997). Basilar-membrane responses to tones at the base of the chinchilla cochlea. *J Acoust Soc Am, 101*, 2151–2163.

Sato, M., Baumhoff, P., Kral, A. (2016). Cochlear implant stimulation of a hearing ear generates separate electrophonic and electroneural responses. *J Neurosci, 36*, 54–64.

Schaefer, S., Sahwan, M., Metryka, A., Kluk, K., Bruce, I. A. (2021). The benefits of preserving residual hearing following cochlear implantation: A systematic review. *Int J Audiol, 60*, 561–577.

Schurzig, D., Pietsch, M., Erfurt, P., Timm, M. E., Lenarz, T., Kral, A. (2021). A cochlear scaling model for accurate anatomy evaluation and frequency allocation in cochlear implantation. *Hear Res*, *403*:108166.

Sellick, P., Patuzzi, R., Robertson, D. (2003). Primary afferent and cochlear nucleus contributions to extracellular potentials during tone-bursts. *Hear Res, 176*, 42–58.

Sijgers, L., Pfiffner, F., Grosse, J., Dillier, N., Koka, K., Röösli, C., Huber, A., Dalbert, A. (2021). Simultaneous intra- and extracochlear electrocochleography during cochlear implantation to enhance response interpretation. *Trends Hear, 25*, 2331216521990594.

Tan, F., Zhu, Y., Ma, Z., Al-Rubeai, M. (2020). Recent advances in the implant-based drug delivery in otorhinolaryngology. *Acta Biomater, 108*, 46–55.

Tejani, V. D., Kim, J. S., Oleson, J. J., Abbas, P. J., Brown, C. J., Hansen, M. R., Gantz, B. J. (2021). Residual hair cell responses in electric-acoustic stimulation cochlear implant users with complete loss of acoustic hearing after implantation. *J Assoc Res Otolaryngol, 22*, 161–176.

Tsuji, J., & Liberman, M. C. (1997). Intracellular labeling of auditory nerve fibers in guinea pig: Central and peripheral projections. *J Comp Neurol, 381*, 188–202.

Yoshimura, H., Moteki, H., Nishio, S. Y., Usami, S. I. (2020). Electric-acoustic stimulation with longer electrodes for potential deterioration in low-frequency hearing. *Acta Otolaryngol, 140*, 632–638.